การผลิตไดเอทิลอีเทอร์โดยการเร่งปฏิกิริยาดีไฮเดรชันของเอทานอลบนตัวเร่งปฏิกิริยาไฮดรอกซีอะพาไทท์/อะลูมินา-ซิลิกา

นางสาวเอื้อมพร มงคลเสริม

วิทยานิพนธ์นี้เป็นส่วนหนึ่งของการศึกษาตามหลักสูตรปริญญาวิศวกรรมศาสตรมหาบัณฑิต
สาขาวิชาวิศวกรรมเคมี ภาควิชาวิศวกรรมเคมี
คณะวิศวกรรมศาสตร์ จุฬาลงกรณ์มหาวิทยาลัย
ปีการศึกษา 2558

PRODUCTION OF DIETHYLETHER BY CATALYTIC DEHYDRATION OF ETHANOL OVER HYDROXYAPATITE/ALUMINA-SILICA CATALYSTS

Miss Auemporn Mongkolserm

A Thesis Submitted in Partial Fulfillment of the Requirements
for the Degree of Master of Engineering Program in Chemical Engineering
Department of Chemical Engineering
Faculty of Engineering
Chulalongkorn University
Academic Year 2015

Thesis Title PRODUCTION OF DIETHYLETHER BY CATALYTIC DEHYDRATION OF ETHANOL OVER HYDROXYAPATITE/ALUMINA-SILICA CATALYSTS
By Miss Auemporn Mongkolserm
Field of Study Chemical Engineering
Thesis Advisor Associate Professor Bunjerd Jongsomjit, Ph.D.

Accepted by the Faculty of Engineering, Chulalongkorn University in Partial Fulfillment of the Requirements for the Master's Degree

....Dean of the Faculty of Engineering
(Associate Professor Supot Teachavorasinskun, D.Eng.)

THESIS COMMITTEE

....Chairman
(Associate Professor Muenduen Phisalaphong, Ph.D.)

....Thesis Advisor
(Associate Professor Bunjerd Jongsomjit, Ph.D.)

....Examiner
(Chutimon Satirapipathkul, D.Eng.)

....External Examiner
(Ekrachan Chaichana, D.Eng.)

เอื้อมพร มงคลเสริม : การผลิตไดเอทิลอีเทอร์โดยการเร่งปฏิกิริยาดีไฮเดรชันของเอทานอลบนตัวเร่งปฏิกิริยาไฮดรอกซีอะพาไทท์/อะลูมินา-ซิลิกา (PRODUCTION OF DIETHYLETHER BY CATALYTIC DEHYDRATION OF ETHANOL OVER HYDROXYAPATITE/ALUMINA-SILICA CATALYSTS) อ.ที่ปรึกษาวิทยานิพนธ์หลัก: บรรเจิด จงสมจิตร, 83 หน้า.

ตัวเร่งปฏิกิรยาไฮดรอกซีอะพาไทท์และอะลูมินา-ซิลิกาที่เตรียมด้วยวิธีทางกายภาพและเคมีถูกทดสอบผ่านปฏิกิริยาการขจัดน้ำของเอทานอลสำหรับการเร่งปฏิกิริยาและค่าการเลือกเกิด ตัวเร่งปฏิกิริยาที่ถูกเตรียมด้วยวิธีทางกายภาพโดยเปลี่ยนแปลงอัตราส่วนโดยน้ำหนักของไฮดรอกซีอะพาไทท์ต่ออะลูมินา-ซิลิกา (ร้อยละ 0-100 โดยน้ำหนัก) ในส่วนของการเตรียมด้วยวิธีทางเคมี, ตัวเร่งปฏิกิริยาไฮดรอกซีอะพาไทท์และอลูมินา-ซิลิกาถูกเตรียมด้วยวิธีโซลเจลและการตกตะกอนร่วม ตัวเร่งปฏิกิยาทั้งหมดจะถูกทดสอบคุณลักษณะด้วยการกระเจิงรังสีเอกซ์ การดูดซับทางกายภาพด้วยไนโตรเจน การส่องผ่านด้วยกล้องจุลทรรศน์อิเล็กตรอน การกระจายตัวของโลหะ การวัดการดูดกลืนแสงอินฟาเรด การคายซับของแอมโมเนียแบบโปรแกรมอุณหภูมิ และการวิเคราะห์การสลายตัวของสารเมื่อได้รับความร้อน การเร่งปฏิกิริยาถูกประเมินผ่านปฏิกิริยาการขจัดน้ำของเอทานอลเพื่อผลิตไดเอทิลอีเทอร์ ปฏิกิริยาถูกทดสอบในสภาวะไอภายใต้ความดันบรรยากาศและที่อุณหภูมิตั้งแต่ 200 ถึง 400 องศาเซลเซียส สำหรับการผลิตไดเอทิลอีเทอร์และสมรรถภาพของการเร่งปฏิกิริยา, time-on-stream ถูกทดสอบที่สภาวะที่เหมาะสมตลอดระยะเวลา 10 ชั่วโมง จากผลการทดลองพบว่าอัตราส่วนโดยน้ำหนักที่เหมาะสมสำหรับตัวเร่งปฏิกิริยาไฮดรอกซีอะพาไทท์ต่ออลูมินา-ซิลิกาเป็น 4 ต่อ 6 โดยน้ำหนักสำหรับวิธีผสมทางกายภาพ ตัวเร่งปฏิกิริยาผลผลิตไดเอทิลอีเทอร์ที่สูงที่สุดร้อยละ 32 ที่อุณหภูมิ 350 องศาเซลเซียส ตัวเร่งปฏิกิริยาที่ถูกเตรียมด้วยวิธีการตกตะกอนร่วมแสดงผลผลิตไดเอทิลอีเทอร์ที่สูงที่สุดที่อุณหภูมิ 300 องศาเซลเซียสเท่ากลับร้อยละ 24

ภาควิชา วิศวกรรมเคมี
สาขาวิชา วิศวกรรมเคมี
ปีการศึกษา 2558

ลายมือชื่อนิสิต ....
ลายมือชื่อ อ.ที่ปรึกษาหลัก ....

5770375921 : MAJOR CHEMICAL ENGINEERING

KEYWORDS: DIETHYL ETHER, ETHYLENE / HYDROXYAPATITE / ALUMINA / SILICA / ETHNOL DEHYDRATION / ACID CATALYST

AUEMPORN MONGKOLSERM: PRODUCTION OF DIETHYLETHER BY CATALYTIC DEHYDRATION OF ETHANOL OVER HYDROXYAPATITE/ALUMINA-SILICA CATALYSTS. ADVISOR: ASSOC. PROF. BUNJERD JONGSOMJIT, Ph.D., 83 pp.

Hydroxyapatite and alumina-silica catalysts prepared by physical and chemical methods were examined in ethanol dehydration reaction for catalytic activity and selectivity. The catalysts prepared by physical mixing method were obtained by varying weight ratios of hydroxyapatite to alumina-silica (0-100 wt%). In chemical mixing method part, the hydroxyapatite and alumina-silica catalysts were prepared by sol-gel and co-precipitation methods. All catalysts were characterized by X-ray diffraction (XRD), N_2 physisorption, scanning electron microscopy (SEM), energy dispersive X-ray spectroscopy (EDX), Fourier Transform Infrared Spectroscopy (FTIR) Analysis, Raman spectroscopy, NH_3-tempearture programmed desorption (NH_3-TPD) and thermal gravimetric analysis (TGA). The catalytic activity was determined in dehydration reaction of ethanol in order to produce diethylether (DEE). The reaction was run in gas phase at atmospheric pressure and temperature range from 200 to 400°C. For DEE production and catalytic performance, time-on-stream was performed at suitable condition during 10 hours. From the result, it was found that the optimal ratio of hydroxyapatite to alumina-silica catalyst was 4 to 6 by weight % for the physical mixing. The catalyst exhibited the highest DEE yield as 32% at 350°C. The catalyst prepared by co-precipitation method presented the highest DEE yield at 300°C as 24%.

Department: Chemical Engineering Student's Signature ....
Field of Study: Chemical Engineering Advisor's Signature ....
Academic Year: 2015

ACKNOWLEDGEMENTS

I would like to impressively thank my thesis advisor, Associate Professor Bunjerd Jongsomjit, Ph.D. for his advice and guidance in order to solve the problem in this research as well as invaluable help, understanding and continued support. I realize the teachings of his. This thesis cannot be achieved without my advisor.

Furthermore, I also have to thank Associate Professor Muenduen Phisalaphong, Ph.D, as a chairman, Dr. Chutimon Satirapipathkul, D.Eng and Dr. Eakrachan Chaichana, D.Eng as the members of the thesis committee for suggestions and taking valuable time to review this thesis.

The authors thank the Thailand Research Fund (TRF), the National Research Council of Thailand (NRCT) and Ratchadaphiseksomphot Endowment Fund (2015) of Chulalongkorn University (CU-58-027- AM) for financial support of this project.

Finally, I most gratefully acknowledge my family, co-worker and my friends in Center of Excellence on Catalysis and Catalytic Reaction Engineering laboratory for all support and carefulness.

CONTENTS

Page

THAI ABSTRACT ... iv

ENGLISH ABSTRACT ... v

ACKNOWLEDGEMENTS ... vi

CONTENTS ... vii

LIST OF TABLES ... 1

LIST OF FIGURES ... 2

CHAPTER 1 INTRODUCTION ... 4

1.1 General Introduction ... 4

1.2 Research objectives ... 7

1.3 Research scopes ... 7

1.4 Research methodology ... 8

CHAPTER 2 THEORIES ... 10

2.1 Ethanol dehydration reaction ... 10

2.2 Hydroxyapatite catalyst ... 12

2.3 Synthesis of catalyst ... 13

CHAPTER 3 LITERATURE REVIEW ... 14

3.1 Dehydration reaction over silica and alumina catalysts ... 14

3.2 Hydroxyapatite-base catalysts ... 15

CHAPTER 4 EXPERIMENTAL ... 18

4.1 Catalyst preparation ... 18

4.1.1 Materials ... 18

4.1.2 Preparation of Al-SSP catalysts ... 18

Page
4.1.3 Preparation of Al-SSP/HAP catalysts by physical mixing 19
4.1.4 Preparation of Al-SSP/HAP catalysts by chemical mixing 19
4.2 Catalyst Characterization 20
4.2.1 ICP analysis 20
4.2.2 Scanning electron microscopy (SEM) and energy X-ray spectroscopy (EDX) 20
4.2.3 X-ray diffraction (XRD) 21
4.2.4 Nitrogen physisorption (BET)..21
4.2.5 Temperature programmed adsorption (NH_3-TPD)..................................21
4.2.6 X-Ray Fluorescence (XRF) 21
4.2.7 Fourier Transform Infrared Spectroscopy (FTIR) Analysis 22
4.2.8 Raman spectroscopy (FT-Raman)..22
4.2.9 Thermo gravimetric analysis (TGA) 22
4.3 Catalytic activity 23
4.3.1 Scheme and procedure..23
4.3.2 Chemicals and reagents 23
4.3.3 Instruments and apparatus...24
4.4 Benefits...24
4.5 Research Plan..25
CHAPTER 5 RESULTS AND DISCUSSION 26
5.1 Comparative study of catalytic activity of HAP/Al-SSP catalysts preparing by physical method...26
5.1.1 Catalyst characterization 26
5.1.2 Catalytic activity test...40

Page

5.2 Investigation of catalytic activity of HAP/Al-SSP catalysts prepared by chemical methods. 44

5.2.1 Catalyst characterization 44

5.2.2 Catalytic activity test 59

5.3 Investigation of catalytic activity of HAP/Al-SSP catalysts for time-on-stream (TOS) during 10 hours. 62

CHAPTER 6 CONCLUSIONS AND RECOMMENDATIONS 67

6.1 Conclusions 67

6.2 Recommendations 68

REFERENCES 70

VITA 83

LIST OF TABLES

Table 2. 1 Main ions in hydroxyapatite body. $[M_{10}(ZO_4)_6X_2]$ 12

Table 4. 1 The chemicals used in the catalysts preparation. 18

Table 4. 2 Nomenclature of all catalysts. 20

Table 5. 1 Textural properties of all catalysts. 28

Table 5. 2 The amount of each element on the surface of all catalysts from EDX. 38

Table 5. 3 The surface acidity of all catalysts from NH_3-TPD. 39

Table 5. 4 Product yield of all catalysts obtained from ethanol dehydration. 43

Table 5. 5 Textural properties of all catalysts. 45

Table 5. 6 The amount of each element on the surface of all catalysts from EDX. 50

Table 5. 7 The surface acidity of all catalysts from NH_3-TPD. 50

Table 5. 8 The composition in geological of all catalysts from XRF. 52

Table 5. 9 The position of chemical groups of catalysts from FT-IR. 55

Table 5. 10 Raman band position of 40H60AS-CS catalyst. 57

Table 5. 11 Raman band position of 40H60AS-CP catalyst. 58

Table 5. 12 Product yield of all catalysts obtained from ethanol dehydration. ...61

Table 6. 1 Product yield of all catalysts obtained from ethanol dehydration. 68

LIST OF FIGURES

Figure 2. 1 Mechanism of ethylene from ethanol. 10

Figure 2. 2 Mechanism of diethylether from ethanol. 11

Figure 2. 3 Products from ethylene in industry [15]. 11

Figure 4. 1 Experimental set-up for reaction test. 23

Figure 5. 1 XRD patterns of all catalysts. 27

Figure 5. 2 Nitrogen adsorption/desorption isotherms of all catalysts. 30

Figure 5. 3 The SEM micrographs of all catalysts. 32

Figure 5. 4 The typical EDX mapping of 100AS catalyst. 33

Figure 5. 5 The typical EDX mapping of 20H80AS-P catalyst. 34

Figure 5. 6 The typical EDX mapping of 40H60AS-P catalyst. 35

Figure 5. 7 The typical EDX mapping of 60H40AS-P catalyst. 36

Figure 5. 8 The typical EDX mapping of 80H20AS-P catalyst. 37

Figure 5. 9 The typical EDX mapping of 100H catalyst. 37

Figure 5. 10 NH_3-TPD profiles of all catalysts. 40

Figure 5. 11 Ethanol conversion of all catalysts at different temperatures. 41

Figure 5. 12 The DEE selectivity of all catalysts at different temperatures. 42

Figure 5. 13 XRD patterns of all catalysts. 44

Figure 5. 14 Nitrogen adsorption/desorption isotherms of all catalysts. 46

Figure 5. 15 The SEM micrographs of all catalysts. 47

Figure 5. 16 The typical EDX mapping of 40H60AS-CS catalyst. 48

Figure 5. 17 The typical EDX mapping of 40H60AS-CP catalyst. 49

Figure 5. 18 NH_3-TPD profiles of all catalysts 51

Figure 5. 19 FTIR spectra of 40H60AS-CS catalyst. 53

Figure 5. 20 FTIR spectra of 40H60AS-CP catalyst. 53

Figure 5. 21 FTIR spectra of 40H60AS-CP catalyst (display chemical groups).........54

Figure 5. 22 FT-Raman spectra of 40H60AS-CS catalyst...56

Figure 5. 23 FT-Raman spectra of 40H60AS-CP catalyst...57

Figure 5. 24 Ethanol conversion of all catalysts at different temperatures............59

Figure 5. 25 DEE selectivity of all catalysts at different temperatures. 60

Figure 5. 26 Ethanol conversion of all catalysts for time on stream 10 h. 62

Figure 5. 27 DEE yield of all catalysts for time on stream 10 h. 63

Figure 5. 28 Thermal gravimetric analysis (TGA) of spent catalysts for time on stream 64

Figure 5. 29 Thermogravimetric and differential thermal analysis of spent catalysts for time on stream 65

CHAPTER 1
INTRODUCTION

1.1 General Introduction

Diethylether (DEE) is a renewable fuel, which presents a high cetane number more than 125. It is necessary to blend with ethanol/bio-ethanol or diesel to improve the performance of diesel engine and reduce emission. DEE is a common product from petrochemicals obtained by petroleum source. It is a clear and colorless liquid using as a solvent for waxes, fats, oils, production of plastic, and etc. including pharmaceutics. Due to the lack of petroleum and global air issue, an alternative energy has been interesting in developing in order to produce the petrochemicals products from non-petroleum source, such as biomass. Ethanol dehydration reaction is an alternative green way to produce DEE. Ethanol as raw material feed, can be converted to DEE, ethylene and acetaldehyde using heterogeneous catalysts [1-3]. Ethanol dehydration reactions (1) and (2) have long been of interest and developed to produce petrochemicals products. As seen, ethylene is a major product at high temperature due to its endothermic reaction, while DEE is preferred at lower temperature as it proceeds via exothermic reaction. Therefore, in order to remain high selectivity of DEE, the ethanol dehydration reaction must be operated at low temperature. As the result, the ethanol conversion would be low, which essentially turns into low DEE yield.

$$CH_3CH_2OH \longrightarrow CH_2{=}CH_2 + H_2O \qquad (1) \qquad \Delta H_{298} = +\ 44.9\ \text{kJ/mol}$$

$$2CH_3CH_2OH \longrightarrow (CH_3CH_2)_2O + H_2O \qquad (2) \qquad \Delta H_{298} = -\ 25.1\ \text{kJ/mol}$$

Solid acid catalysts, especially having strong BrØnsted acid sites must be required in order to have a high catalytic activity. Acid catalysts protonate hydroxyl groups, which leave molecules of water. Then, it deprotonates methyl groups and hydrocarbon rearranges into ethylene, which is endothermic reaction [4, 5]. In case of DEE, it represents by two different pathways as associative and dissociative pathways. The associative pathway adsorbs two molecules of alcohol. Then, it directly establishes DEE. The dissociative pathway adsorbs first molecule of alcohol following by water elimination. Then, it adsorbs alkyl group and water. The alkyl group and second alcohol engender DEE [4]. Maintaining temperature in reaction is strongly maintaining yield of product as mentioned above.

Hydroxyapatite (HAP) is a major composition of skeleton. The stoichiometry of the hydroxyapatite is 1.50-1.67 by Ca/P ratio. An oxygen atom of the free -OH group is coordinated to three calcium cations [6]. Characteristics of the catalyst depend on the Ca/P ratio including substitution of component ions. It shows active area with both of weak acid and basis sites in a single-crystal lattice, which are essential property for dehydration reaction [6, 7]. Non-stoichiometric of HAP with loss of calcium presents difference of catalyst characteristics. With Ca/P molar ratio of 1.5, the catalyst exhibits the acidic property. As a basic catalyst, the Ca/P molar ratio is 1.67 [5]. Takashi et al. (2006) studied HAP catalyst in ethanol dehydration reaction. Various products are obtained with HAP catalyst in ethanol dehydration including ethylene, DEE, 1,3 butadiene, buthanol, olefins, propylene, aromatic and etc. Moreover, products also depend on temperature and contact time. Ethanol is converted into DEE at low temperature with low Ca/P ratios of HAP catalyst. In 2008, they continuously studied the HAP catalyst by varying reaction temperature. They reported that the products are strongly dependent on reaction temperature [8, 9]. According to the report of Rahmanian et al. [5], they found that hydroxyapatite and alumina catalyst with (Ca+Al)/P molar ratio of 1.62 exhibited a high catalytic activity for ethanol dehydration to produce DEE.

Alumina and silica catalysts are widely used as catalyst. Alumina catalysts have a high surface acidity together with BrØnsted and Lewis site. The property of alumina catalysts is varied with different types such as ϒ-Al_2O_3, X-Al_2O_3 and mixed phase ϒ-X-Al_2O_3 catalysts. Phillips Oil Company used ϒ-Al_2O_3 treated with KOH and ZnO/Al_2O_3 in ethanol dehydration reaction to produce ethylene. Doheim et al. [10] investigated alumina doped with Na_2O and Mn_2O_3 presenting 97% ethanol conversion at 300^{o}C. The catalyst was added by $Ti(SO_4)_2$ and Na2CO3. The result showed high ethylene selectivity up to 99% at 500^{o}C. Although the alumina catalysts can be used in ethanol dehydration reaction and produced ethylene product, the reaction temperature is still high including other products are formed. Silica catalysts process a high activity in dehydration reaction. It is frequently used with normal metal and exhibits very high surface area, suitable acidity and high thermal stability. Jiménez-Morales et al. examined silica catalysts doped with zirconium and impregnated with sulphuric acid. The mesoporous silica catalyst existing Zr exhibited an acid solid catalyst. Luts and Katz [11] studied silica catalyst on self-supported reacting with ethanol. Ethane was obtained at high reaction temperature.

In order to improve activity and characteristics of the catalysts in ethanol dehydration reaction, alumina is used to cooperate with silica. Pérez et al. [12] reported that silica promoted alumina mesophases presented a high acid property and surface area. Phung and Busca [13] used the commercial catalysts in ethanol dehydration reaction. It is produced both of ethylene and DEE between temperatures from 423 to 723 K. DEE formation being more favored for lower Si/Al ratios. The DEE and ethylene selectivity depend on the nature of the active site. Chanchuey et al. [14] investigated alumina-silica catalysts doped with Mo in dehydration reaction of ethanol. Assembling alumina and silica without Mo presented the lowest amount of acid site that is preferred in ethanol dehydration. Adding Mo in the catalysts achieved the highest conversion as 100%.

In the present work, hydroxyapatite/alumina-silica catalysts are investigated for their characteristics and performance to be used in ethanol dehydration reaction to obtain DEE. The preparation of catalysts including physical and chemical (sol-gel and precipitation) methods is compared to determine the most effective way to prepare the highly potential hydroxyapatite/alumina-silica catalysts for DEE production.

1.2 Research objectives

To study the catalytic performance of hydroxyapatite catalyst for the dehydration reaction of ethanol to diethylether.

1.3 Research scopes

- To Prepare hydroxyapatite catalyst mixing with alumina-silica (Al-SSP) solid acid catalyst by physical and chemical methods by varying ratios of two components.
- To test the catalytic activity of dehydration reaction of ethanol under atmospheric pressure at temperature from 200°C to 400°C.
- To test the catalytic performance under optimal condition in order to produce diethylether in the ethanol dehydration reaction.
- All catalysts are characterized by X-ray diffraction (XRD), N_2 physisorption, scanning electron microscopy (SEM) and energy dispersive X-ray spectroscopy (EDX), temperature-programmed desorption of ammonia (NH_3-TPD) and ICP analysis.

1.4 Research methodology

Part I: The effect of HAP/Al-SSP ratio on catalytic activity by physical mixing method for the ethanol dehydration reaction

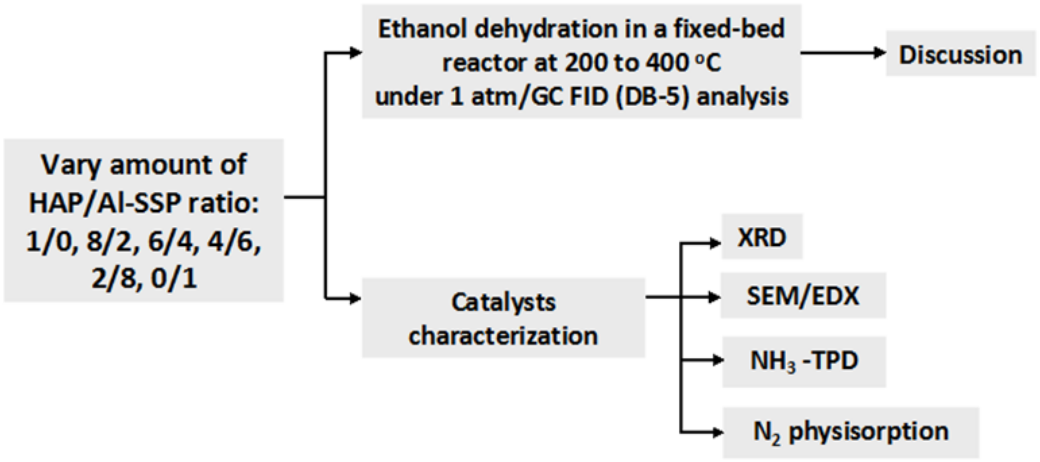

Part II: The effect of HAP/Al-SSP ratio on catalytic activity by chemical mixing method for the ethanol dehydration reaction

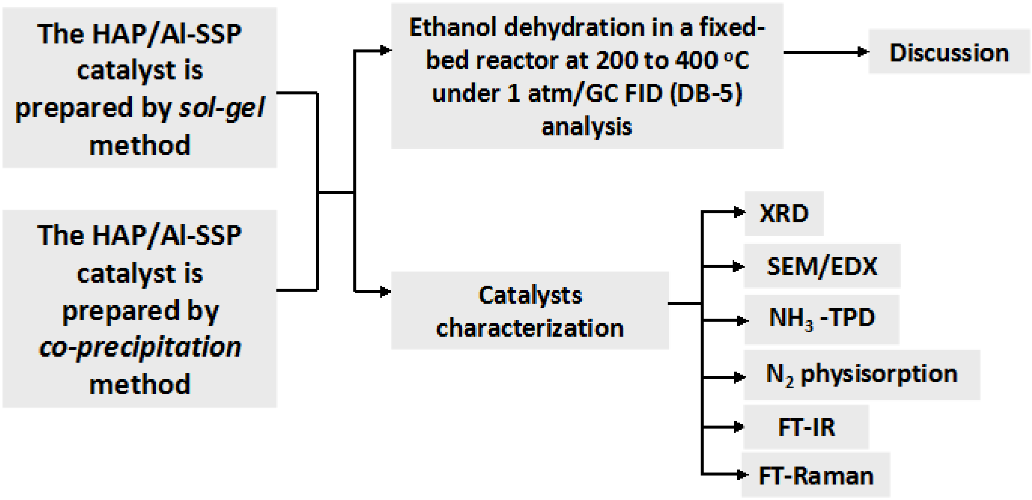

CHAPTER 2

THEORIES

2.1 Ethanol dehydration reaction

Dehydration reaction of ethanol has been produce ethylene and diethylether. According to figure 2.1(a) and 2.1(b). It has one and two path way to produce ethylene and diethylether, respectively [4]. Ethylene is a main product of the dehydration. Dithylehter is usually obtained at low temperature, ethylene is reverted. The dehydration of ethanol is carried out in gas phase in fixed-bed reactor over various acid catalysts. The dehydration reaction require both BrØnsted and Lewis acidity of catalyst outstanding catalytic activity. Many studies report the effect of conditions in reaction and catalysts on the ethanol conversion and product selectivity.

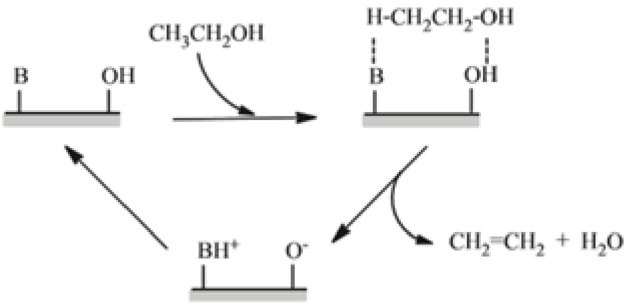

Figure 2. 1 Mechanism of ethylene from ethanol.

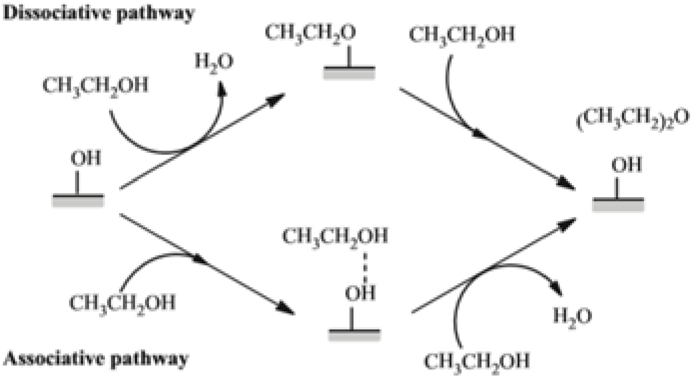

Figure 2. 2 Mechanism of diethylether from ethanol.

Ethylene is widely use as a precursor of plastic and polymer such as polyethylene, ethylene dicholoride, ethyleneoxide, ethylbenzene, etc [15]. Diehtylether is a volatile solvent, clear colorless, also known as ether and ethoxyethane. Diethylether is a general use as a solvent in laboratory, as a precursor in pharmaceutical and a valuable chemical for clean fuel. It can be synthesis both in industry and laboratory. The reaction have to occur in low temperature obtaining high product yield.

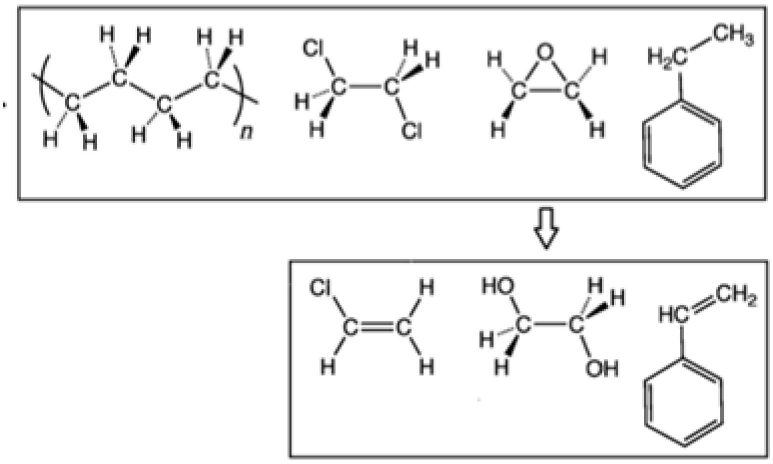

Figure 2. 3 Products from ethylene in industry *[15].*

2.2 Hydroxyapatite catalyst

Hydroxyapatite is a calcium phosphate in a main element of skeleton. An important component in a hard tissue of human. It is mostly used as bio-materials in medical. Structure in body of hydroxyapatite consist of various element described by Yasushi Suetsuguas a formula $M_{10}(ZO_4)_6X_2$. Property of hydroxyapatite rely on molar ratio of calcium and phosphate, also element in structure [16].

Table 2. 1 Main ions in hydroxyapatite body. [$M_{10}(ZO_4)_6X_2$]

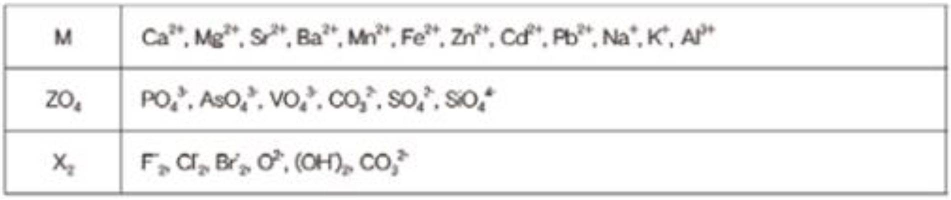

M	Ca^{2+}, Mg^{2+}, Sr^{2+}, Ba^{2+}, Mn^{2+}, Fe^{2+}, Zn^{2+}, Cd^{2+}, Pb^{2+}, Na^{+}, K^{+}, Al^{3+}
ZO_4	PO_4^{3-}, AsO_4^{3-}, VO_4^{3-}, CO_3^{2-}, SO_4^{2-}, SiO_4^{4-}
X_2	F^-_2, Cl^-_2, Br^-_2, O^{2-}, $(OH)^-_2$, CO_3^{2-}

Hydrooxyapatite present any application descrobed by Nidhi Kanthari [17]

- Bone tissue engineering
- Bone void fillers for orthopaedic, traumatology, spine, maxillofacial and dental surgery.
- Orthopedic and dental implant coating
- Restoration of periodontal defects
- Edentulous ridge augmentation
- Endodontic treatment like pulp capping
- Repair of mechanical furcation perforations and apical barrier formation
- Fillers for reinforcing restorative glass ionomer cement (GIC) and restorative composite resin

- Desensitizing agent in post teeth bleaching
- Remineralizing agent in toothpastes
- Early carious lesions treatment
- Drug and gene delivery

2.3 Synthesis of catalyst

- *Sol-gel method*

A sol is a dispersion of particles in a solvent. In the solvent may be have both of crystallize and amorphous of particles. A gel consist of liquid phase and particular gel established to build a network

- The idea behind sol-gel synthesis is to "dissolve" the compound in a liquid in order to bring it back as a solid in a controlled manner.

- Multi component compounds may be prepared with a controlled stoichiometry by mixing sols of different compounds.

- The sol-gel method prevents the problems with co-precipitation, which may be inhomogeneous, be a gelation reaction.

- Enables mixing at an atomic level.

- Results in small particles, which are easily sinterable.

- *Co-precipitation method*

Co-precipitation is precipitation separating an element down from a solution. According to BY I. M. KOLTHOFF [18] co-precipitation is separated by

- The amount of sample is obtained within an impurities during precipitation.

- An impurities are adsorbed during composition is carrying down.

- The amount of mixture precipitate by the adsorption on surface area.

CHAPTER 3
LITERATURE REVIEW

3.1 Dehydration reaction over silica and alumina catalysts

Yong Tae Kim, et al. (2011) [19] investigated the silica-alumina catalyst on the dehydration reaction of glycerol by varying Si/Al molar ration. All catalysts were prepared by the co-precipitation method. The specific surface areas of the catalysts became significantly larger with increasing an amount of the mole fraction of Al. The peak intensity of XRD increased when the amount of Si was increased up to 0.8. Analysis if surface acidity from NH_3-TPD found that the total amount of acid sites increased when increasing the mole fraction of Si up to 0.6 and decreased with a future increase. From catalytic activity, the dehydration reaction was strongly depended on the acid property and products yield was proportional to the concentration of the BrØnsted and Lewis acid sites.

PèreBy L, et al. (2014) [12] studied about the effect of SiO_2 addition in alumina on the structural and textural properties. Different precursor of SiO_2:TEOS and Ludox® established the propertied of catalysts. The highest surface area and a high density of weak Lewis acid sites were obtained by using TEOS-base material. Ludox®-base material provided the smaller pore and reduced the total pore volume.

Thanh Khoa Phung, et al. (2014) [20] started by commercial alumina catalysts and silica-alumina catalyst: P90, P200, V200, D100 and SA330. They found all of catalysts have the type IV of porosity characteristic. From pyridine adsorption, P200 and V200 had strong Lewis acid sites which P200 had the strongest site. The only SA330 catalysts (silica-alumina) had both very strong Lewis sites and BrØnsted sites. In ethanol dehydration reaction test, the total conversion was obtained at 673 K over all of alumina catalysts. The catalytic activity of P200 was higher than SA330 followed by P90 and V200, respectively. Those catalysts gave ethylene yield above 99% at 623 K except V200. Over all of catalysts gave high diethylether selectivity at low temperature and conversion, while temperature and conversion vary directly to the ethylene selectivity.

Phung and Busca (2015) [13] investigated five commercial silica-alumina acid catalysts: one of pure alumina (A), one of pure silica (S) and three of different silica-alumina ratio (SA5, SA30 and SA87). They presented both of strong Lewis and BrØnsted acidity from the characteristic of pyridine adsorption. From BET analysis, the (S) acid catalyst had surface area higher than the (A) acid catalyst but less active. In case of silica-alumina acid catalysts, the catalytic activity was higher correspond to the surface area. Moreover, the catalytic activity of silica-alumina acid catalysts was higher by increasing silica-alumina ratio. However, they founded that the significant difference of diethylether and ethylene seletivities were quite similar conversion.

3.2 Hydroxyapatite-base catalysts

Takashi Tsuchida, et al (2006) [8] prepared hydroxyapatite catalysts by the preciptiation method by varying the Ca/P ratio. The temperature of ethanol dehydration reaction was experimented between 300 to 450^{o}C. BET surface area of each catalysts was 30-50 m^2/g. Hydroxyapatite catalysts had both of a large amount of acid sites and a few of base sites. With low Ca/P ratio (1.52) at low temperature, diethylether was produced. When temperature reached to 400^{o}C, the selectivity of ethylene was 80% and also a small amount of acetaldehyde was produced. By increasing the Ca/P ratio (1.69), n-butanol was produced with the highest selectivity and also acetaldehyde with 24.9% selectivity.

Shuhei Ogo, et al (2012) [21] reported the dehydration reaction of ethanol in fix-bed reactor under atmospheric pressure at 300°C. All of catalysts were pretreated in Ar flow for 3 h under temperature at 550°C. The products were collected in liquild phase for analysis on a GC-FID. Strontinum phosphate hydroxyapatite catalysts with various Sr/P molar ratios from 1.58 to 1.70 were synthesized by hydro-thermal method. From ICP analysis, the Sr/P molar ratios were founded that the molar ratios as 1.67 while increasing a amount of Sr/P ratios in the preparation step. The CO_2 and NH_3 TPD was determined to measure acid and basic sites. The catalysts had strong and weak basic sites. When the Sr/P molar ratios increased the strong basic site also increased. The NH_3-TPD showed that had a large amount of weak acid sites. In case of strong acid sites relatively with increasing in the Sr/P molar ratio. In this study, 1-butanol was mainly produced from the ethanol dehydration reaction. With a small increasing Sr/P molar ratio, the selectivity of 1-butanol was increased and 1-butanol selectivity also depend on ethanol conversion. Moreover, the catalytic activity correspond to the density of strong basic sites.

A. Rahmanian and H.S. Ghaziaskar (2013) [5] compared the effect of adding and non-adding $AlPO_4$ in hydroxyapatite catalyst on ethanol dehydration reaction. The catalysts were prepared by precipitation method with 1.62 Ca/P and 1.62 (Ca+Al)/P molar ratios. A quantity of Ca, P and Al were obtained by EDX analysis. All of characteristics by the BET method of $AlPO_4$/HAP was higher than pure HAP. The results of catalytic testing over HAP catalyst was founded that increasing the temperature diethylether was increased. At 350°C, the diethylether selectivty was highest at 70% while ethanol conversion was gained 38%. After using hydroxyapatite catalyst for 41 h, the catalyst remain stable confirming by the result of XRD analysis.

Yumiko Matsuura, et al (2014) [22] reported hydroxyapatite catalyst for dehydration reaction with various cations and anions (Ca-P, Sr-P, Pb-P, Ca-V and Sr-V). The hydroxyapatite catalysts were obtained by hydrothermal method. Atomic ratios of catalysts were equal to 1.67 except Pb-P hydroxyapatite catalyst (1.71). Specifis surface areas of catalysts was depend on the chemical compositons which the highest was Ca-P hydroxyapatite catalyst. From CO_{2-}TPD analysis, all of catalysts showed that they had a large number of weak basic sites at 350 K. The density of CO_2-TPD method at 500 K increasing in the following by Pb-P, Sr-V, Ca-V and Ca-P, Sr-P. The acid sites was determined by NH_3-TPD increasing in the following by Ca-V, Sr-V, Ca-P, Sr-P and Pb-P and the basic sites was reverse. The catalytic activity reported by dehydrogenation/dehydration ratio. Pb-P and Ca-V catalysts showed the dehydrogenation/dehydration ratio 5.7 and 0.5 respecting to the most amount of basic and acid sites, respectively.

M. Sudhakar, et al (2016) [23] investigated the hydroxyapatite supported metal (Pd, Pt, Ru ,Cu and Ni) catalysts for hydrogenation reaction. The hydroxyapatite supported metals were prepared by a wet impregnation method. The BET surface area of pure hydroxyapatite was highest following by Ru-, Pd-, Cu-, Pt-, and Ni-impregnated. Focused on Ru/HAP, the addintion of Ru affected to the decrease in weak and moderate basic sites while increasing strong basic sites and presented weak, moderate and strong acid sites. Thus, the Ru/HAP catalyst had both of acid and basic sites.

CHAPTER 4

EXPERIMENTAL

4.1 Catalyst preparation

4.1.1 Materials

Table 4. 1 The chemicals used in the catalysts preparation.

Materials	Formula	Supplier
Ethanol (99.99%)	C_2H_5OH	VWR
Tetraethyl orthosilicate (TEOS) (98%)	$Si(OC_2H_5)_4$	Aldrich
Cetyltrimethylammonium bromide (CTAB) (98%)	$CH_3(CH_2)_{15}N(Br)(CH_3)$	Aldrich
De-ionized water	-	-
Ammonia (30%)	NH_3	Panreac
Ammonium nitrate nonahydrate (98%)	$Al(NO_3)_3 \bullet 9H_2O$	Aldrich
Hydroxyapatite (HAP) (Reagent grade)	$Ca_5(OH)(PO_4)_3$	Aldrich
Ruthenium (III)	$Ru(NO)(NO_3)_x(OH)_y$, x+y=3	Aldrich

4.1.2 Preparation of Al-SSP catalysts

According to Chanchuey T, et al. [14] the experiment started by mixing a 11.46 ml of ammonia solution in a 70.56 ml of DI water adding in a 3.3 g of CTAB. Then, the mixture was stirred by magnetic bar for 30 min at room temperature followed by adding a 6.3 g of TEOS and continuous stirred for 1 hr. After that, 16.89 g of $Al(NO_3)_3{\bullet}9H_2O$ was added into the mixture and continuous stirred for 1 hr. Until the white wet-cake was obtained. After that the solution was operated under vacumn condition and dried at room temperature for a day before dried at 110°C overnight. Finally, the solid acid catalyst is calcined under atmospheric pressure at 700°C for 6 hr in air. The Al-SSP is gained as the Al-SSP ratio as 60/40.

4.1.3 Preparation of Al-SSP/HAP catalysts by physical mixing

Firstly, the Al-SSP solid acid catalyst from previous synthesis was mixed with hydroxyapatite (20-80 wt%) in toluene at room temperature and stirred for 40 min. Then, the solvent was removed from the mixture and washed by de-ionized water. The solid catalyst was dried at 110°C overnight and calcined at 600°C for 2 hours in air under atmospheric pressure. The solid catalysts were prepared by varying weight ratios of hydroxyapatite:Al-SSP as 1:0, 2:8, 4:6, 6:4, 8:2, and 0:1 defined by 100H, 20H80AS-P, 40H60AS-P, 60H40AS-P, 80H20AS-P, and 100AS respectively.

4.1.4 Preparation of Al-SSP/HAP catalysts by chemical mixing

- Sol-gel method

The preparation is similar to the Al-SSP catalyst preparation. First, the mixture of 3.3 g of CTAB, 3.2 g of HAP, 11.46 ml of NH_3 and 0.56 ml of DI water was stirred for 30 min at room temperature. Then, 6.3 g of TEOS was added and continuous stirred for an hour. 16.89 g of $Al(NO_3)_3$•$9H_2O$ was added to the solution and continuous stirred for an hour. After white precipitation was obtained, the mixture was filtered under vacuum pump. Then, the Al-SSP/HAP was dried at room temperature for a day and continuous dried at 110°C overnight. In impurity removing step, the catalyst was calcined in air under atmospheric pressure at 700°C for 6 hours. Finally, the Al-SSP/HAP was obtained with the Al-SSP/HAP ratio of 6/4. The catalyst was defined by 40H60AS-CS.

- Co-precipitation

According to Kiyoshi Okada, et al. [24] the method started by mixing 3.3 g of CTAB, 3.2 g of HAP and 16.89 g of $Al(NO_3)_3$•$9H_2O$ in 200 ml of ethanol solution. Then, 6.3 g of TEOS was added into the solution and stirred at room temperature for 3 hours. After that, 100 ml of ammonia solution was added to the solution. After the white co-precipitation was obtained, the sample was dried at room temperature for a day. Finally, the mixture was dried at 110°C for 12 hours before the catalyst was calcined in air at 700°C for 6 hours. The catalyst was defined by 40H60AS-CP.

4.1.5 Nomenclature of catalysts

- **XHYAS-Z** X refer to the weight of hydroxyapatite (HAP)
  Y refer to the weight of alumina-silica (Al-SSP)
  Z refer to the method of catalyst preparation

Table 4. 2 Nomenclature of all catalysts.

Name	HAP/(Al-SSP)	Method
100AS	0	physical
20H80AS-P	20/80	physical
40H60AS-P	40/60	physical
60H40AS-P	60/40	physical
80H20AS-P	80/20	physical
100H	1	physical
40H60AS-CS	40/60	Sol-gel
40H60AS-CP	40/60	Co-precipitation

4.2 Catalyst Characterization

4.2.1 ICP analysis

A quantity of elemental composition in catalysts was analyzed. First, mixing 2.5 ml of nitic acid (HNO_3), following by 1.5 ml of hydrogen peroxide (H_2O_2) and 0.3 ml of hydrochlorie (HCl). 0.1 g of catalyst (HAP) was added in the mixture and stirred for 1 day. Then, the volume was adjusted in a 100 ml of volumetric flask with de-ionized water.

4.2.2 Scanning electron microscopy (SEM) and energy X-ray spectroscopy (EDX)

The morphology and particle size were analyzed to obtain of an element composition in catalyst from several locations by scanning electron microscopy (SEM) with JEOL mode JSM-6400 and energy dispersive X-ray spectroscopy (EDX) with stand Link Isis series 300 program, respectively.

4.2.3 X-ray diffraction (XRD)

A SIEMENS D-5000 X-ray diffractometer with CuK$_{\alpha}$ (λ= 1.54439 Å) was used in order to identify the crystalline phase of all catalysts. The spectra was scanned at a rate of 2.4° min^{-1} in the range of 2 theta equal to 10°-90°.

4.2.4 Nitrogen physisorption (BET)

To calculate surface area, average pore diameter, pore size distribution were measured by N_2 physisorption with a Micromeritics ASAP 2000 automated system. A sample was dried at 110°C for a day before the measurement took place.

4.2.5 Temperature programmed adsorption (NH_3-TPD)

The surface acidity was determined by temperature programmed adsorption (NH3-TPD) using Micromeritics Chemisorp 2750 Pulse Chemisorption System. 0.05 g of catalyst was loaded on 0.03 g of quartz wool in a glass tube. Afterward, the sample was preheated at 650°C under helium flow and saturated with 15%NH3/He for 30 min. Then, the experiment removed any adsorbed NH_3 from 40°C to 650°C. Finally, all TCD peak was measured as a function of temperature.

4.2.6 X-Ray Fluorescence (XRF)

In order to examine element and chemical analysis the X-ray fluorescence spectrometer was performed using Panaanalytical MINIPAL4 analyzer. The 1 g sample was used.

4.2.7 Fourier Transform Infrared Spectroscopy (FTIR) Analysis

FT-IR analysis was used to determine the functional group as the chemical structure of activated carbon using a Nicolet 6700 FTIR spectrometer.

4.2.8 Raman spectroscopy (FT-Raman)

To identify the function of material the Raman spectroscopy was performed. 0.05 g sample was tested in Fourier Transform Raman Spectrometer (FT-Raman) using Neodymium Yttrium Aluminium Garnet (Nd-YAG, wavelength 1,064 nm)

4.2.9 Thermo gravimetric analysis (TGA)

To measure the carbon content in catalyst. Thermo gravimetric analysis: TGA was performed using TA Instruments SDT Q 600 analyzer. The samples of 10-20 mg and a temperature ramping from 298 to 1273 K at 2K/min were used in the operation. The carrier gas was N_2 UHP.

4.3 Catalytic activity

4.3.1 Scheme and procedure

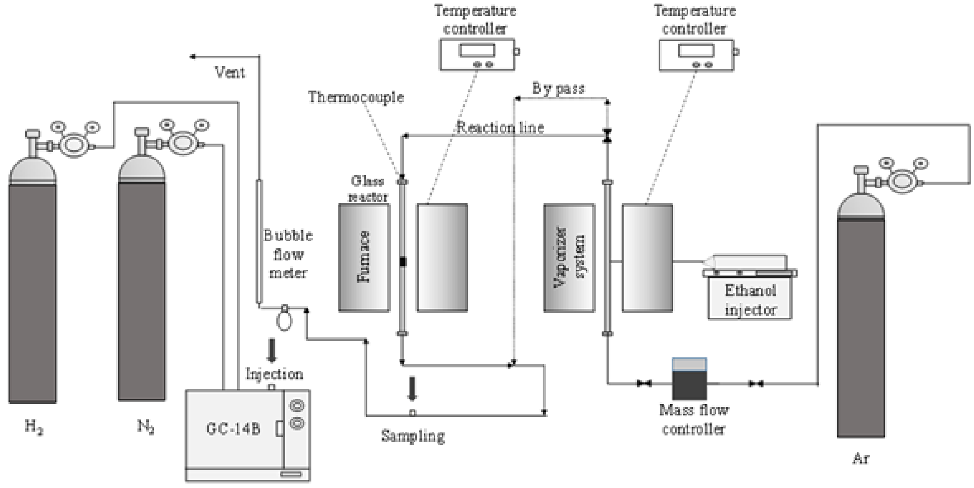

Figure 4. 1 Experimental set-up for reaction test.

The dehydration reaction of ethanol was investigated in fixed bed reactor with an inner diameter 0.7 cm as shown in Figure 4.1. In an experiment, the 0.05 g of solid catalyst was loaded with 0.01 g of quartz wool into the reactor. First, the solid catalyst was treated with 60 ml/h of Argon under atmospherics pressure at 200°C for 1 h. Then, a vaporized ethanol was fed into the reactor. The catalytic activity was tested at 200-400°C under atmospherics pressure and the products were analyzed by the Shimadzu GC8A gas chromatograph with FID using capillary column (DB-5) at 150°C. Finally, the conversion and selectivity of ethanol dehydration were collected.

4.3.2 Chemicals and reagents

- High purity grade hydrogen gas (99.999%) (TIG)
- Ultra high purity nitrogen gas (99.999%) (TIG)
- Ultra high purity argon gas (99.999%) (TIG)
- Absolute ethanol (99.8%) (VWR CHEMICALS)

4.3.3 Instruments and apparatus

- Reactor: The reactor is made from glass tube which is borosilicate type with an inside diameter of 0.7 mm.
- Vaporizer: The ethanol feed is vaporized at the temperature of 120°C under atmospheric pressure. The boiling point of ethanol is 78.37°C.
- Gas system: Argon/N_2 is a carrier gas. It carries the ethanol feed into reactor controlling by adjusting a pressure regulator with 2.5 bar and mass flow controller at 1.45 ml/h.
- Temperature controller:
    - At furnace, the temperature is set at temperatures in range between 200°C to 400°C.
    - At vaporizer, the temperature is set at 120°C. (Above the boiling point of product from ethanol dehydration)
- Gas chromatography (GC): A Gas chromatography is used for investigating ethanol conversion and product selectivity. It equipped (Shimadzu GC-14B) with flame ionization detector (FID) with DB-5 capillary column. The operating condition for gas chromatography is reported;
    - Detector: FID
    - Capillary column: DB-5
    - Carrier gas: Nitrogen (99.99 vol. %) and Hydrogen (99.99 vol. %)
    - Column temperature: Initial 40°C, Final 40°C
    - Injector temperature: 150°C
    - Detector temperature: 150°C
    - Time analysis: 8 min
    - Analyzed gas: ethanol, ethylene, diethyl ether, acetaldehyde

4.4 Benefits

- It obtains various catalysts for dehydration of ethanol.
- This study is an alternative for catalysts in ethanol dehydration reaction.

- It can realize the different properties of the catalysts.

4.5 Research Plan

Activity	2015-2016											
	Jul	Aug	Sep	Oct	Nov	Dec	Jan	Feb	Mar	Apr	May	June
1. Literature Reviews	←	—	—	—	—	→						
2. Chemical purchasing	↔											
3. Preparation catalysts and Characterization of catalysts				←	—	—	—	—	—	→		
4. Perform the ethanol dehydration reaction					←	—	—	—	—	—	→	
5. Discussion and Conclusion							←	—	—	—	—	→

CHAPTER 5
RESULTS AND DISCUSSION

In this chapter, the results and discussion of HAP/Al-SSP catalysts are explained on characteristics and catalytic activities. All catalysts were prepared by physical and chemical methods as following in chapter 4. The catalytic activity was performed in ethanol dehydration reaction at temperature range from 200°C to 400°C and attempt to find optimal condition in order to produce DEE. The characteristics are indicated by nitrogen physisorption, temperature programmed adsorption (NH_3-TPD), X-ray diffraction (XRD), scanning electron microscopy (SEM) and energy dispersive x-ray spectroscopy (EDX), X-ray fluorescence (XRF), Fourier Transform infrared spectroscopy (FTIR) analysis and Raman spectroscopy including thermal gravimetric analysis (TGA) on the investigation of stability. The results and discussion is divided into 3 parts, comparative study of catalytic activity of HAP/Al-SSP catalysts prepared by physical method, investigated catalytic activity of HAP/Al-SSP catalysts prepared by chemical methods and investigation of catalytic stability of HAP/Al-SSP catalysts.

5.1 Comparative study of catalytic activity of HAP/Al-SSP catalysts preparing by physical method.

All catalysts were preparing by physical method and varying amount of HAP and Al-SSP in catalysts (0-100 wt%).

5.1.1 Catalyst characterization

5.1.1.1 X-ray diffraction (XRD)

According to crystal structure analyses performed by X-ray diffraction (XRD), a pure and well-crystallized 100H catalyst was obtained with only one phase [25]. The pure HAP catalyst flourished sharp peaks at 26, 30, 32, 33, 40, 47 and 49° following

Figure 5.1. The pure Al-SSP catalyst showed broad peaks at 21-24° identifying the amorphous structure of silica. Likewise, sharp peaks at 45 and 67° were indicated by ϒ-Al_2O_3 structure [14]. Moreover, other mixing catalysts exhibited both of sharp peaks at 25-35, 45 and 67° and broad peaks at 21-24° representing the crystallite structure of hydroxyapatite, alumina and silica. In according with figure sharp peaks of hydroxyapatite showed clear overs other that result from well-crystallized structure must great-display on X-ray diffraction (XRD) analysis.

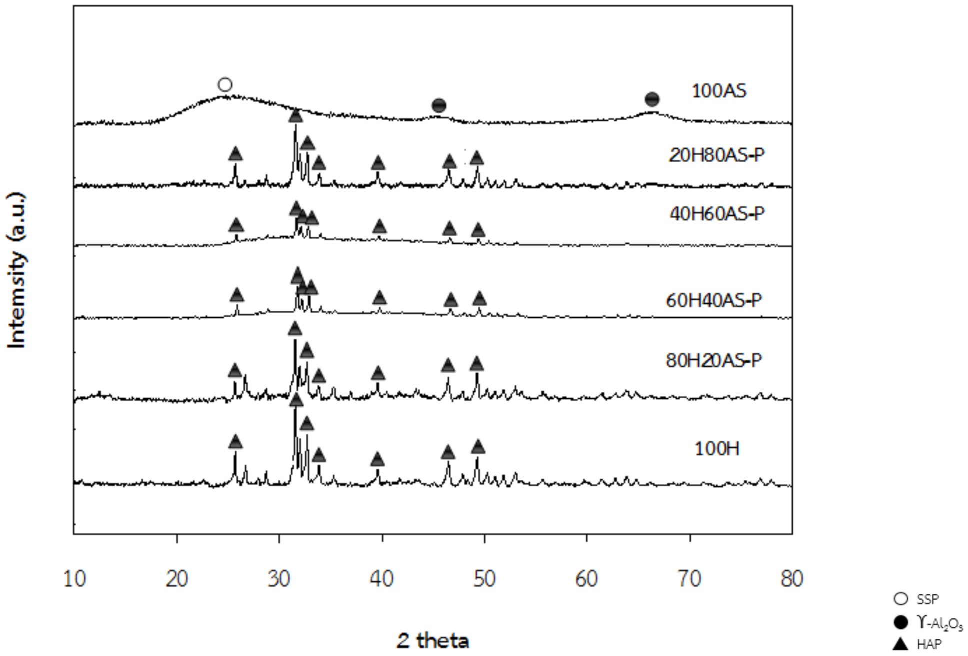

Figure 5. 1 XRD patterns of all catalysts.

5.1.1.2 Nitrogen physisorption

The BET surface area, average pore size diameter and average pore volume are summarized in Table 5.1. 100AS catalyst presents the highest the BET surface area of 276 (m^2/g). Increasing amount of HAP decreased the BET surface area, due to HAP blocked on Al-SSP surface and volume. The least BET surface area as 4 (m^2/g) is 100H that significantly non-porous and inactive in ethanol dehydration reaction. Average pore volume and pore size diameter of all mixing HAP/Al-SSP catalysts is similar. Average pore volume of all catalysts is about 0.1-0.4 (cm^3/g). Average pore size diameter of all mixing catalysts is 6-7 nm that specifying mesoporous catalyst. 100H is non-porous.

Table 5. 1 Textural properties of all catalysts.

Catalyst	BET surface area S_{BET} (m^2/g)	Average pore size diameter (nm)	Average pore volume (cm^3/g)
100H	4	11.3	0.0
20H80AS-P	168	6.4	0.3
40H60AS-P	120	6.8	0.2
60H40AS-P	72	6.3	0.1
80H20AS-P	41	6.5	0.1
100AS	276	5.6	0.4

From N_2 adsorption-desorption isotherms analysis, the results are shown in Figure 5.2. According to IUPAC classification, all catalysts submit Type IV isotherms excepting for 100H. The Type IV isotherms is representative of mesoporous catalyst that related to average pore size diameter. Besides, the mesoporous-typical catalyst is well-characteristics on ethanol dehydration reaction [12].

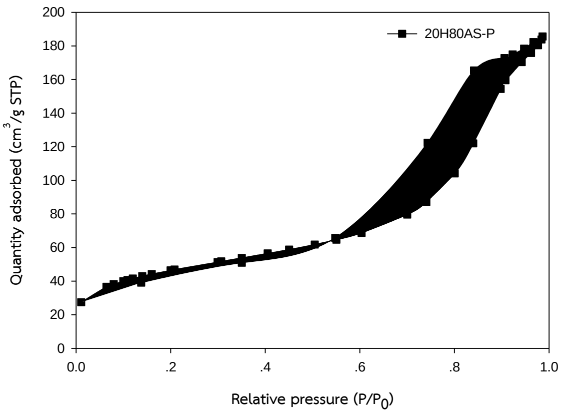
20H80AS-P
Quantity adsorbed (cm^3/g STP)
0
20
40
60
80
100
120
140
160
180
200
0.0
.2
.4
.6
.8
1.0
Relative pressure (P/P$_0$)

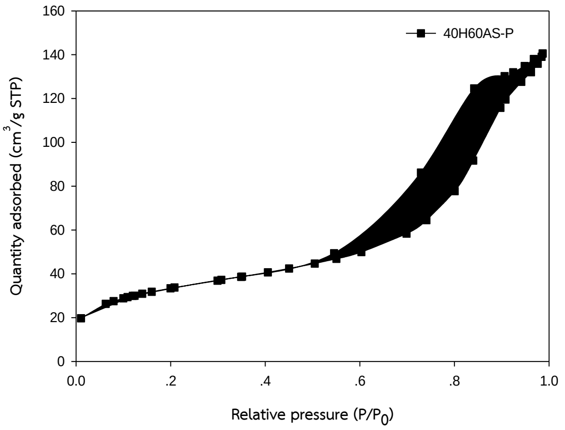
40H60AS-P
Quantity adsorbed (cm^3/g STP)
0
20
40
60
80
100
120
140
160
0.0
.2
.4
.6
.8
1.0
Relative pressure (P/P$_0$)

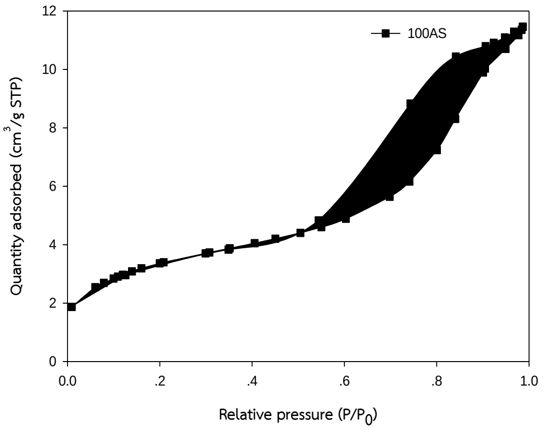
100AS
Quantity adsorbed (cm^3/g STP)
0
2
4
6
8
10
12
0.0
.2
.4
.6
.8
1.0
Relative pressure (P/P$_0$)

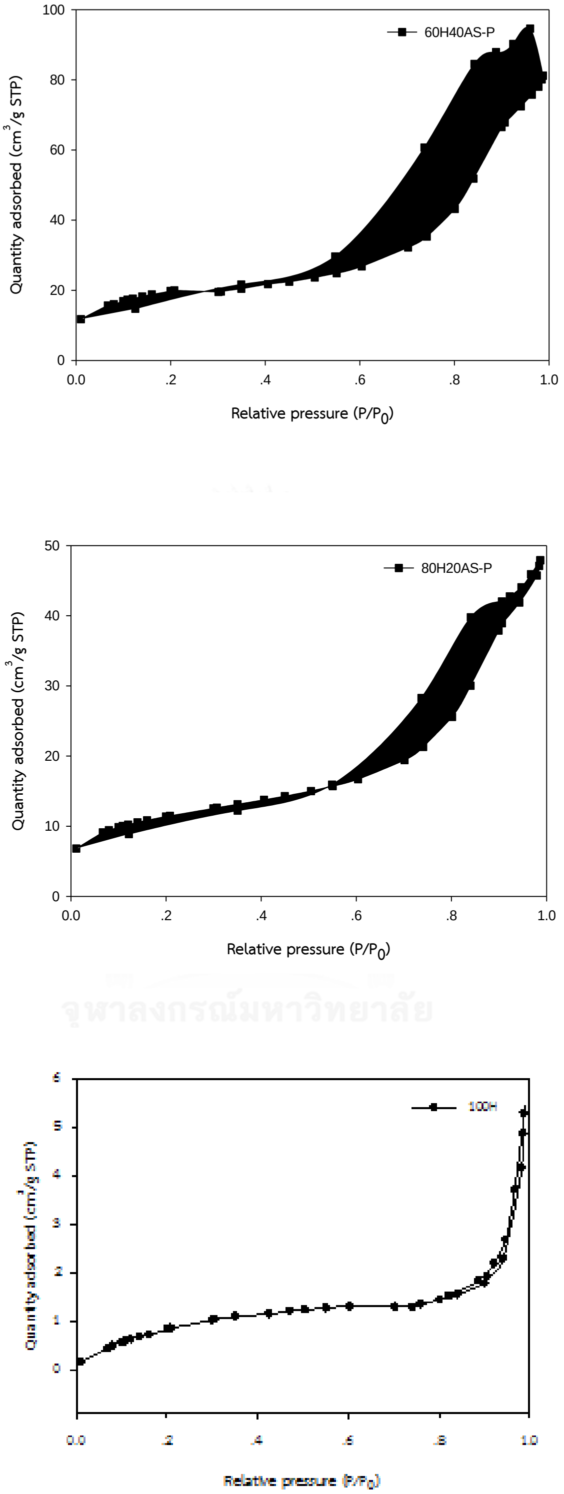

Figure 5. 2 Nitrogen adsorption/desorption isotherms of all catalysts.

5.1.1.3 Scanning electron microscopy (SEM) and energy dispersive X-ray spectroscopy (EDX)

All catalysts were identified the morphology by SEM as shown in Figure 5.3. The morphology of 100AS catalyst was obviously spheroidal having the average particle size around 0.4-0.5 microns. The addition of HAP would change the morphology as shown in Figure 5.3. The morphology of mixing catalysts were smaller than 100AS having the average particle size less than 0.3 microns. The particle size of 100H catalyst was seen with also less than 0.3 microns.

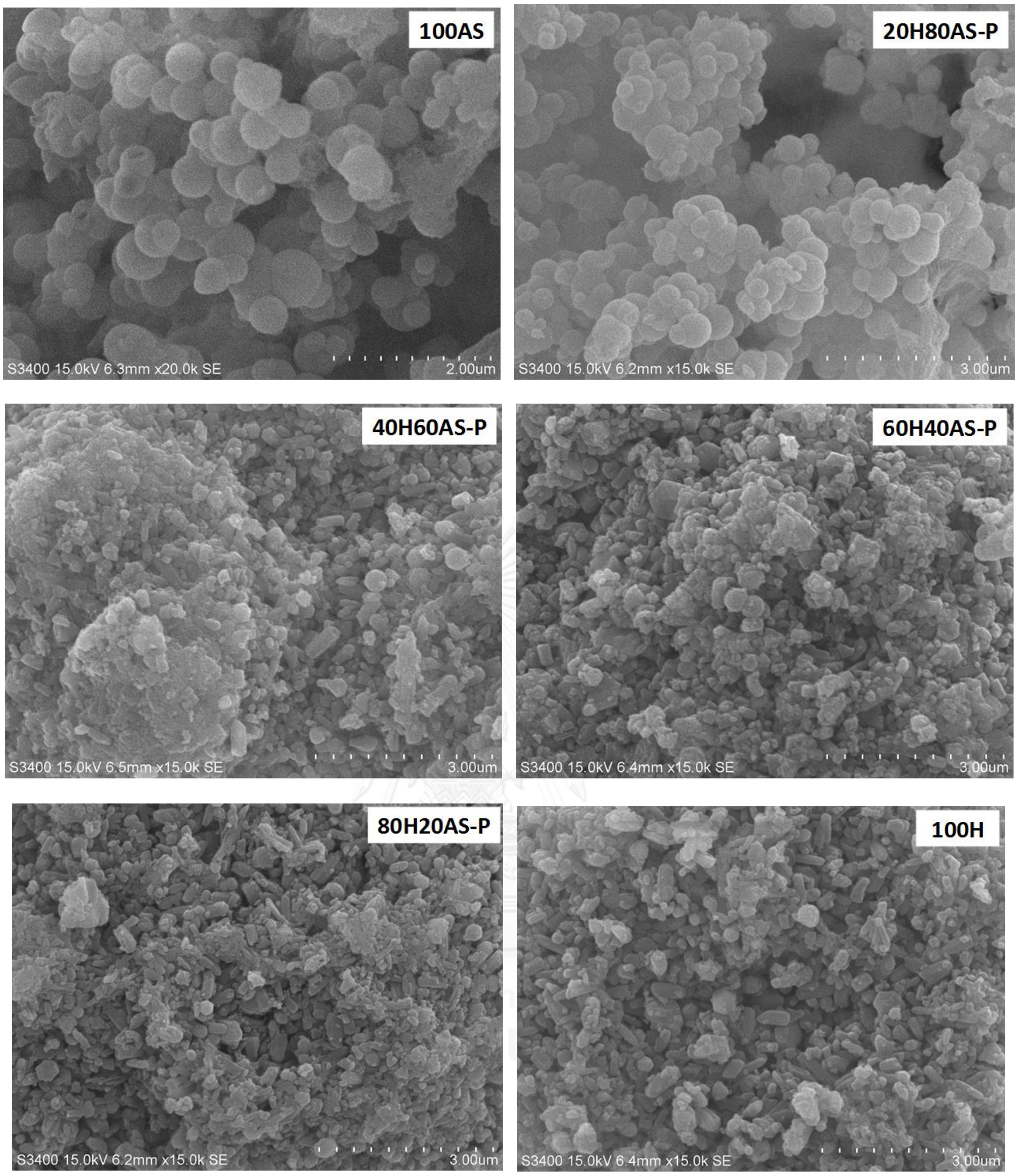

Figure 5. 3 The SEM micrographs of all catalysts.

The element distribution in all catalysts were detected by energy dispersive x-ray spectroscopy (EDX) method. The element composition of 100AS catalyst consists of Al, Si and O. The 100H catalyst is comprised of P and Ca as shown in Figure 5.4 & 5.9. According to Figure 5.5-5.8, all elements (Al, Si, O, P and Ca) present in all mixing catalysts. Each of element can be seen by the color dots on the photograph with addition amount of HAP, the density of P and Ca was obvious seen and well distribution.

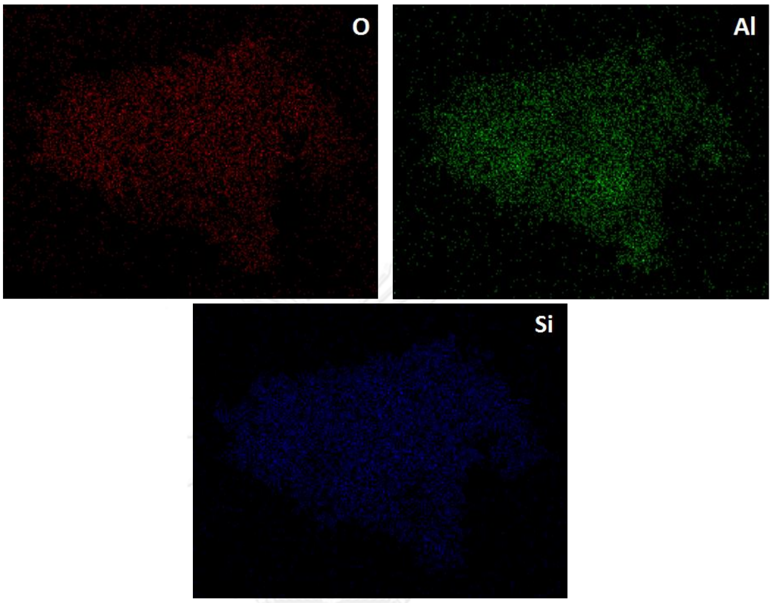

Figure 5. 4 The typical EDX mapping of 100AS catalyst.

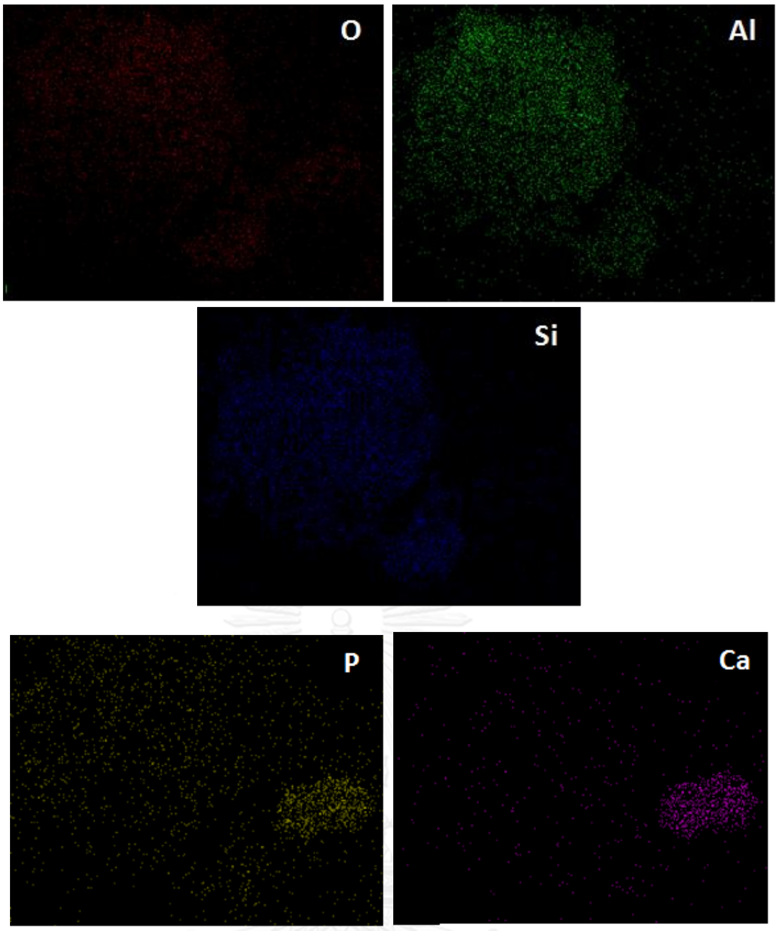

Figure 5. 5 The typical EDX mapping of 20H80AS-P catalyst.

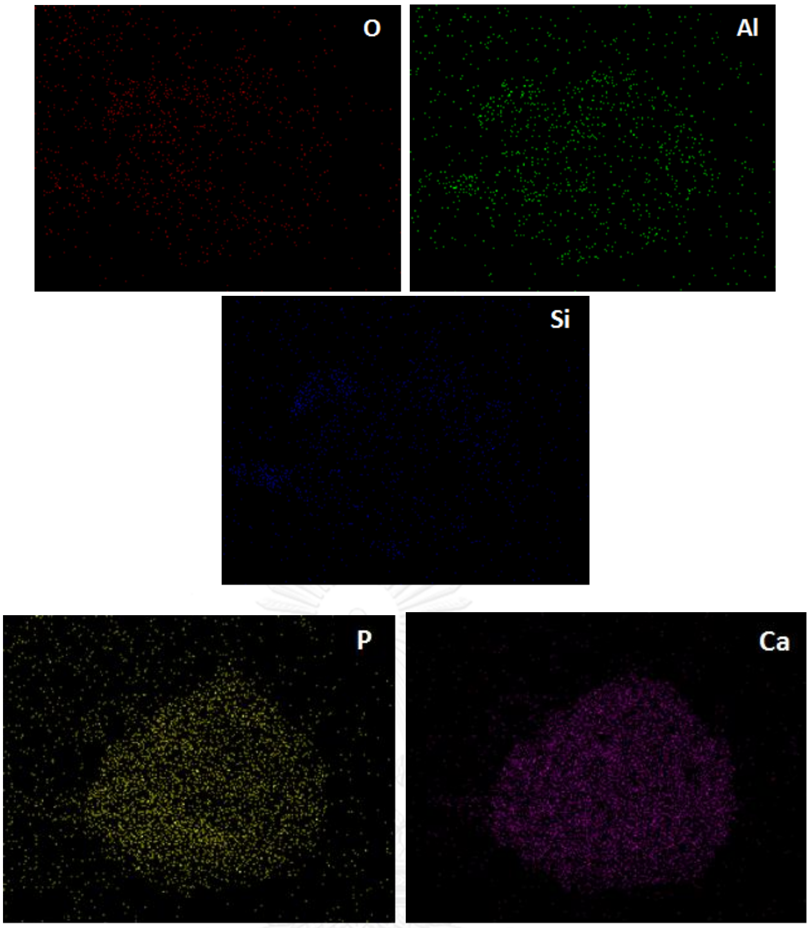

Figure 5. 6 The typical EDX mapping of 40H60AS-P catalyst.

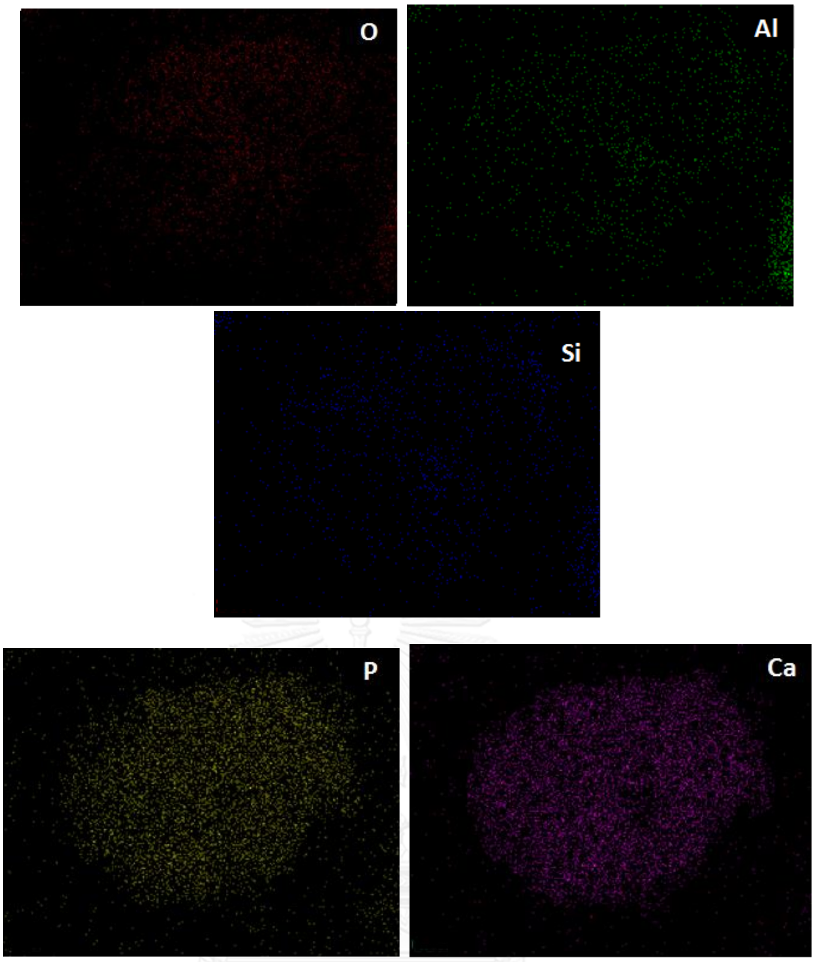

Figure 5. 7 The typical EDX mapping of 60H40AS-P catalyst.

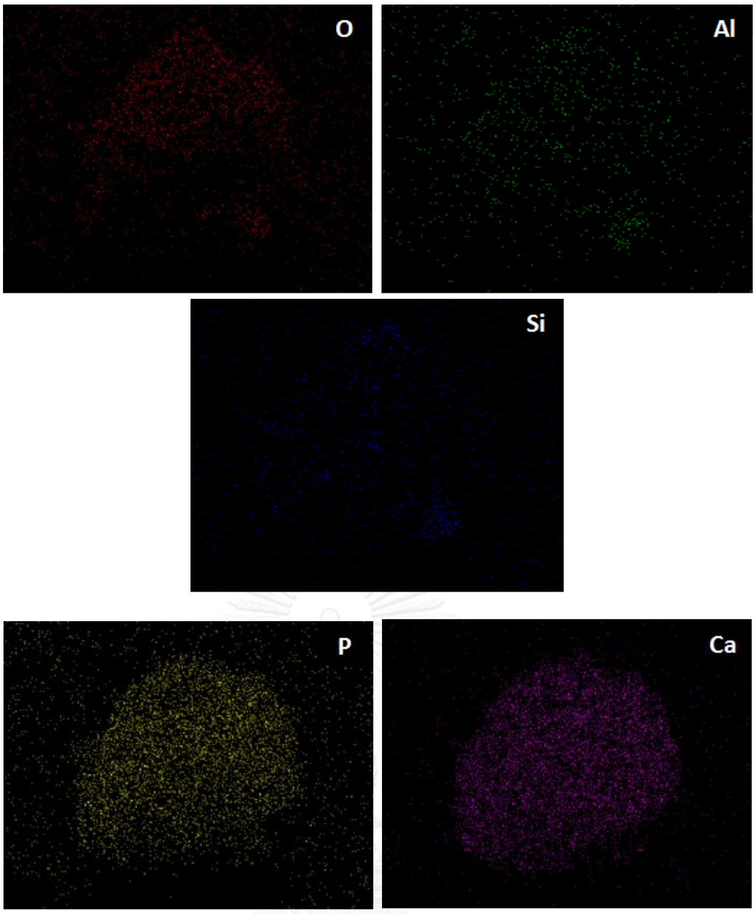

Figure 5. 8 The typical EDX mapping of 80H20AS-P catalyst.

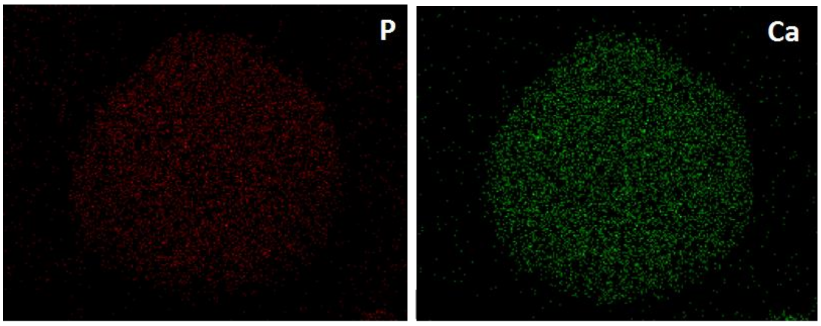

Figure 5. 9 The typical EDX mapping of 100H catalyst.

Moreover, the quantity of each element near the surface of catalyst can also be measured by EDX. The results are summarized in Table 5.2. The amount of Ca and P of all mixing catalysts obtaining from EDX were less than the amount of loading except for the 40H60AS-P catalyst. Thus, the catalytic activity may be dependent on the location of catalyst.

Table 5. 2 The amount of each element on the surface of all catalysts from EDX.

Catalysts	**Amount of element on surface (wt%)**				
	Ca	**P**	**Al**	**Si**	**O**
100AS	-	-	19.5	30.7	49.8
20H80AS-P	4.4	10.7	18.1	23.5	43.3
40H60AS-P	42.5	19.0	2.6	4.1	31.8
60H40AS-P	31.5	21.4	5.0	5.3	36.8
80H20AS-P	33.3	21.7	2.0	1.7	41.3
100H	63.1	36.9	-	-	-

5.1.1.4 Temperature programmed adsorption (NH_3-TPD)

The surface acidity was determined by temperature-programmed desorption (NH_3-TPD). Table 5.3 shows the acid property of all catalysts. The 100AS catalyst exhibits the largest of surface acidity of 1518.1 μ mole/g.cat. The decreasing surface acidity is proportional to increasing the amount of HAP. The least acid property is 100H as 61.2 μ mole/g.cat. Considering on 20H80AS-P and 40H60AS-P catalysts, there are similar amount of surface acidity. However, 40H60AS-P catalyst displays weak-moderate acid sites more than 20H80AS-P catalyst that prefers to produce DEE [26, 27].

Table 5. 3 The surface acidity of all catalysts from NH_3-TPD.

Catalysts	Number of acid sites (μ mole/g.cat)			
	Weak acid sites	**Moderate acid sites**	**Strong acid sites**	**Total acid site**
100AS	572.2	572.2	373.7	1518.1
20H80AS-P	151.6	318.5	334.3	804.4
40H60AS-P	78.5	466.3	186.0	730.8
60H40AS-P	326.0	189.2	124.2	639.4
80H20AS-P	136.9	146.4	149.3	432.6
100H	15.2	22.5	23.5	61.2

The TPD profile is shown in Figure 5.10. All catalysts exhibit one desorption peak below 250°C. There is weak acid sites qualification. The number of weak acid sites are proportion to area below curve that is related to results in Table 5.3. The desorption peak form 250°C to 400°C is refered to moderate to strong acid sites. The number of this acid site are gradually decreased following the Table. Generally, weak acid site can be identified BrØnsted acid site. Lewis acid site is refered to the strong acid site. Eventually, the BrØnsted acid site is preferred in dehydration reaction of ethanol [14, 26, 28].

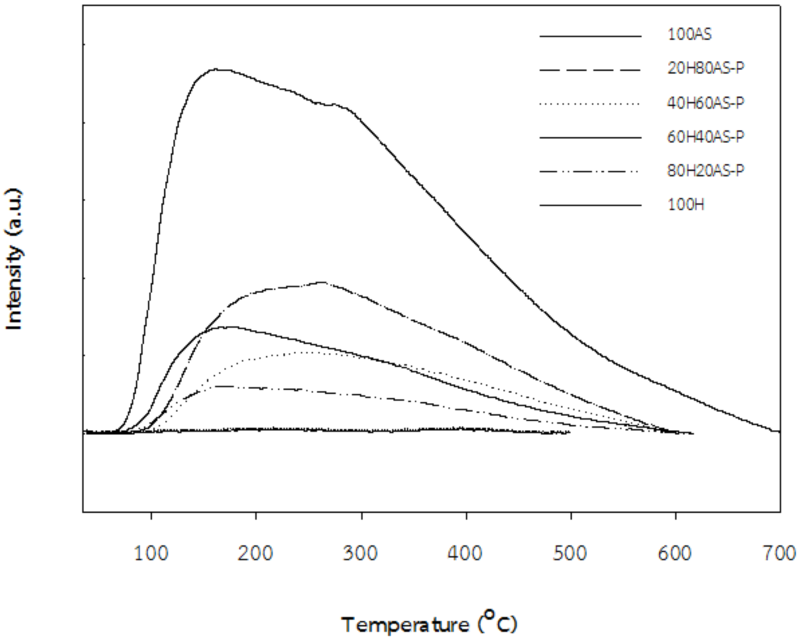

Figure 5. 10 NH_3-TPD profiles of all catalysts.

5.1.2 Catalytic activity test

To determine the catalytic activity of ethanol dehydration, all catalysts were investigated. Ethanol dehydration reaction was performed at atmospheric pressure with temperature range from 200 to 400°C. First, 0.05 g of catalyst was added into continuous flow micro-reactor. Then, treating with 60 ml/min of argon for one hour. Follow by testing in dehydration reaction of ethanol in gas phase. Finally, all products gas was analyzed gas chromatograph with FID. From experimental, the results are shown in Figure 5.11. All catalysts presented, ethanol conversion increased while increasing operating temperature. No significant ethanol conversion was found at temperature below 350°C. Ethanol conversion of the addition of HAP decreased with increased amount of HAP, which was related to the total number of acid site. The catalytic activity of ethanol dehydration relies on the surface acidity. From these results, 40H60AS-P catalyst exhibited the highest ethanol conversion among all mixing catalysts. The 40H60AS-P catalyst exhibits the largest total amount of acid site. Thus, the acid property of catalyst is an important key influencing on product selectivity and ethanol conversion.

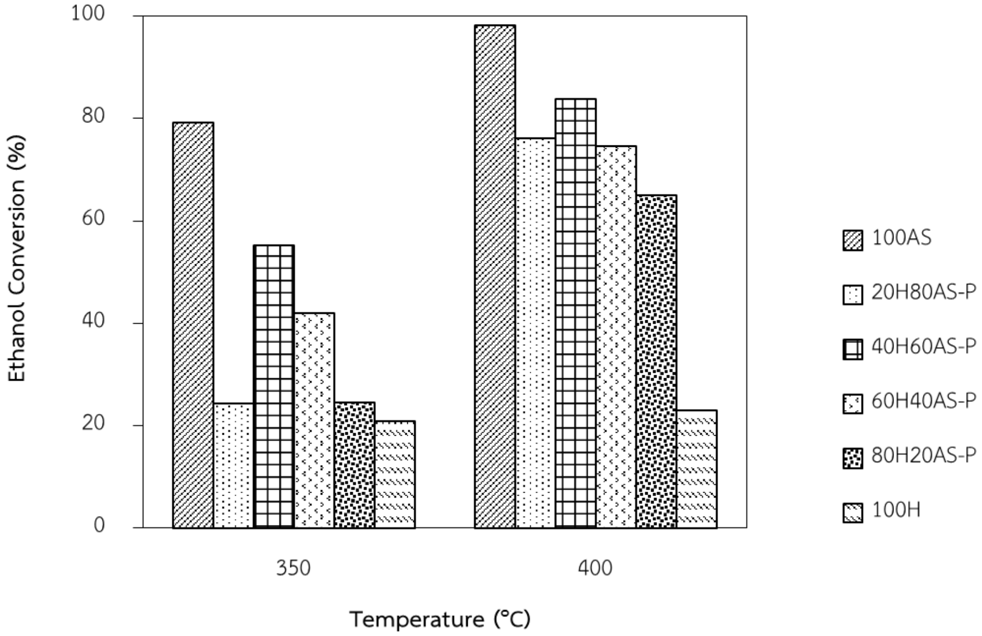

Figure 5. 11 Ethanol conversion of all catalysts at different temperatures.

According to Figure 5.12 , DEE is the major product at low temperature (350°C), while at high temperature (400°C) ethylene is principle. Acetaldehyde could not be produced over all these catalysts. At low temperature, the DEE selectivity of all mixing catalysts is similar and rapidly decreased at higher temperature. In order to produce DEE low temperature is required. This is according to thermodynamic properties that the DEE production is exothermic reaction. The DEE selectivity of 100H was more than that of 100AS. Therefore, addition of 100H into AS is favor to produce DEE.

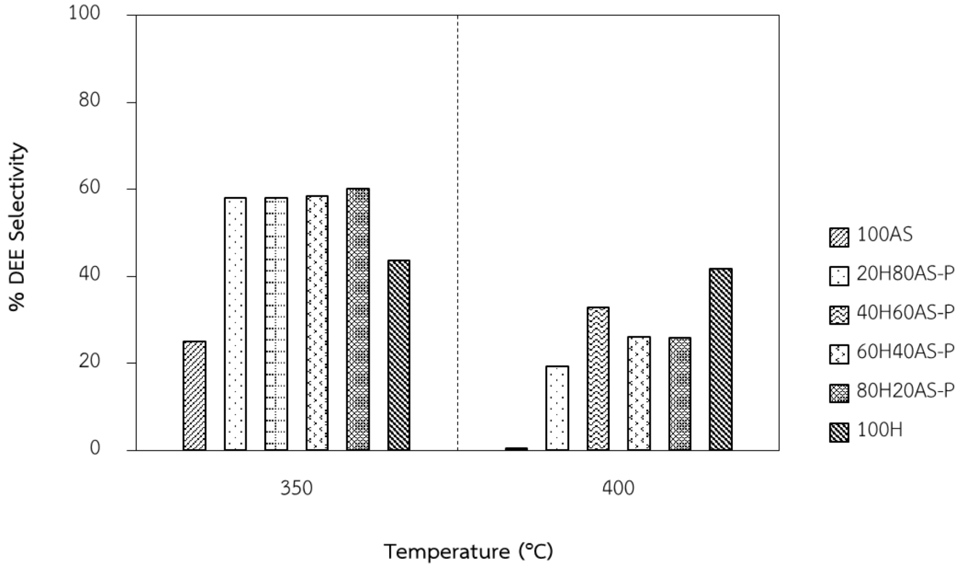

Figure 5. 12 The DEE selectivity of all catalysts at different temperatures.

DEE yields are summarized in Table 5.4. Considering for DEE yield at low temperature (350°C), all mixing catalysts can be produced DEE larger than pure catalysts (100AS and 100H). This is because of mixing catalysts having weak-moderate acid sites more than strong acid site. It is confirmed that the amount of surface acidity mainly affected to ethanol conversion and DEE selectivity including DEE yield. The highest DEE yield of 32.1% is obtained from 40H60AS-P catalyst with optimal condition on reaction at 350°C.

Table 5. 4 Product yield of all catalysts obtained from ethanol dehydration.

Catalyst	% Yield (350°C)		% Yield (400°C)	
	Ethylene	DEE	Ethylene	DEE
100AS	59.2	19.8	97.6	0.4
20H80AS-P	10.2	14.1	61.3	14.7
40H60AS-P	23.0	32.1	55.9	27.6
60H40AS-P	17.3	24.6	54.8	19.5
80H20AS-P	9.7	14.7	47.8	16.9
100H	6.8	9.2	10.6	9.6

5.2 Investigation of catalytic activity of HAP/Al-SSP catalysts prepared by chemical methods.

Two catalysts were prepared by sol-gel and co-precipitation methods having HAP/Al- SSP weight ratio of 4/6.

5.2.1 Catalyst characterization

5.2.1.1 X-ray diffraction (XRD)

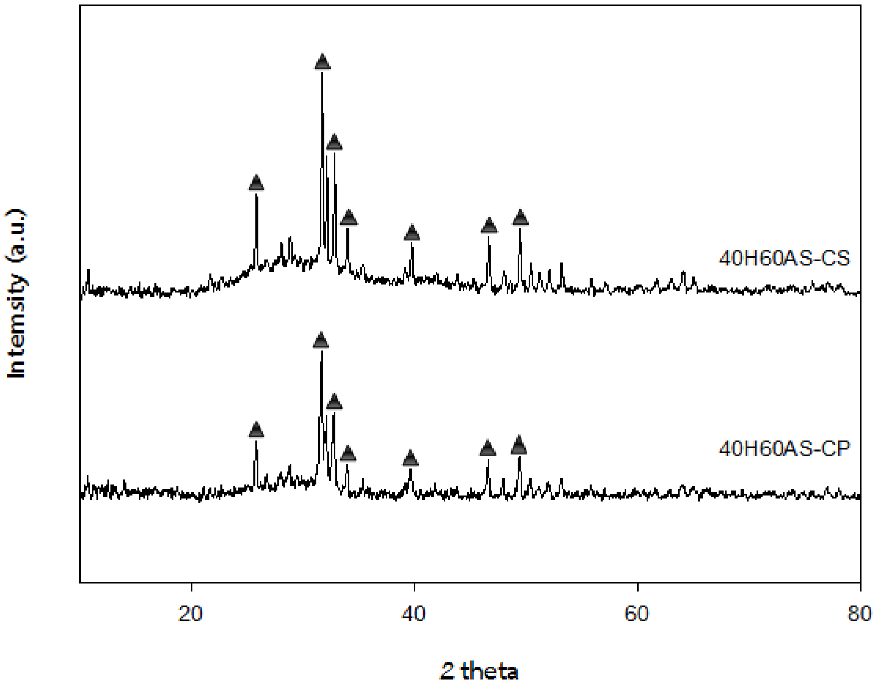

Figure 5. 13 XRD patterns of all catalysts.

XRD patterns of 40H60AS-CS and 40H60AS-CP catalysts are shown in Figure 5.13. Both catalysts show pure-crystallize sharp peaks of HAP at 26, 30, 32, 33, 40, 47 and 49^{o} [29], [25]. Although catalysts have alumina and silica, they did not display in the Figure. This is due to X-ray diffraction analysis prefers analyze crystallize structure to amorphous structure.

5.2.1.2 Nitrogen physisorption

BET surface area, average pore size diameter and average pore volume are summarized in Table 5.5. The BET surface area of 40H60AS-CS and 40H60AS-CP is 191 and 228 (m^2/g), respectively. The 40H60AS-CP has a larger BET surface than 40H60AS-CS. The result shows that co-precipitation method gives better textural property than sol-gel method. Both 40H60AS-CS and 40H60AS-CP catalysts prepared by chemical method have BET surface area larger than 40H60AS-P prepared by physical method. Thus, catalysts prepared by chemical methods exhibit better property that may affect the catalytic activity in ethanol dehydration. Average pore volume of 40H60AS-CS and 40H60AS-CP catalysts is similar having the value of 0.4 (cm^3/g), which is higher two times than that of 40H60AS-P catalyst. Average pore size diameter obtained (4-6 nm) for 40H60AS-CS and 40H60AS-CP catalyst indicates the mesoporous catalyst.

Table 5. 5 Textural properties of all catalysts.

Catalyst	BET surface area S_{BET} (m^2/g)	Average pore size diameter (nm)	Average pore volume (cm^3/g)
40H60AS-CS	191	6.0	0.4
40H60AS-CP	228	4.3	0.4

From N_2 adsorption-desorption isotherm experiment, the results are shown in Figure 5.14. According to IUPAC classification, both catalysts exhibit Type IV isotherms that are related to the result of average pore size diameter. By reason of Type IV isotherms is agent of mesoporous material.

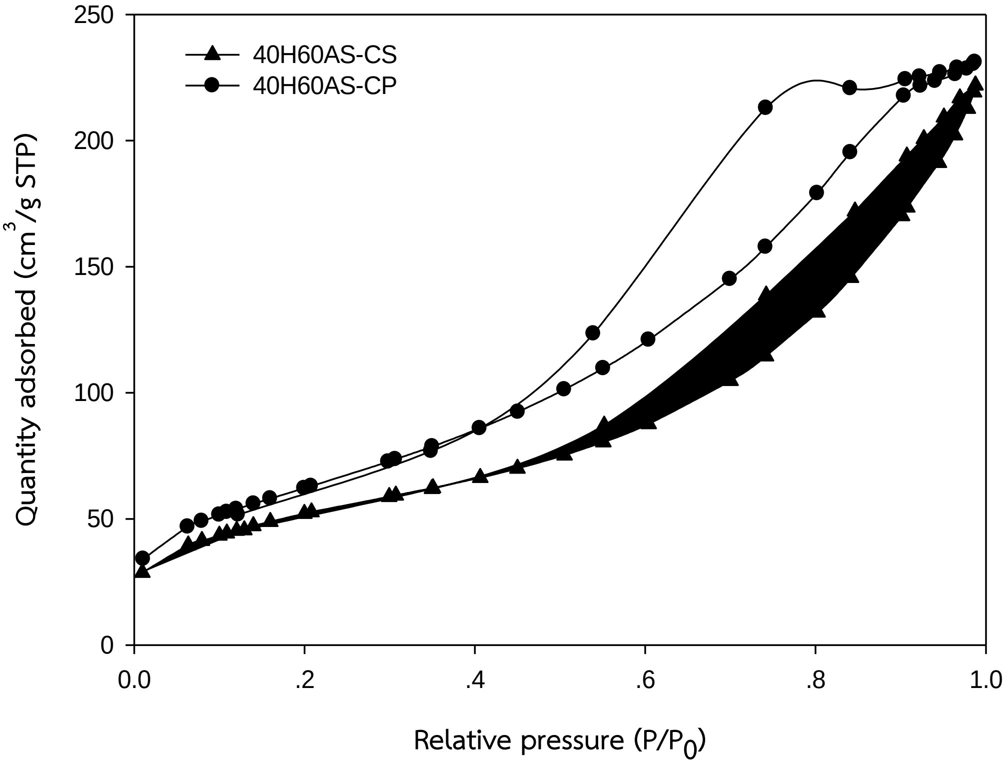

Figure 5. 14 Nitrogen adsorption/desorption isotherms of all catalysts.

5.2.1.3 Scanning electron microscopy (SEM) and energy dispersive x-ray spectroscopy (EDX)

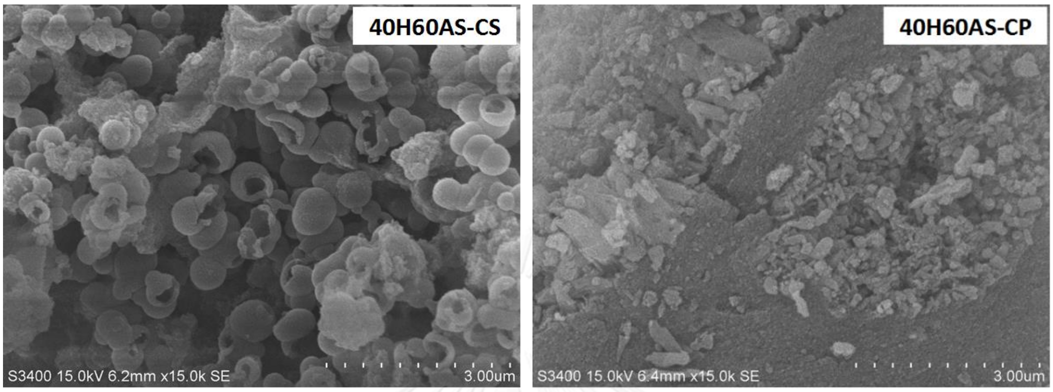

Figure 5. 15 The SEM micrographs of all catalysts.

SEM micrographs of 40H60AS-CS and 40H60AS-CP catalysts obtained are shown in Figure 5.15. The morphology of 40H60AS-CS catalyst was semi-circular particle having average particle size around 0.5-0.6 microns. The 40H60AS-CP catalyst had smaller particle size than 40H60AS-CS with average particle size of 0.1-0.3 microns and non-spherical shape.

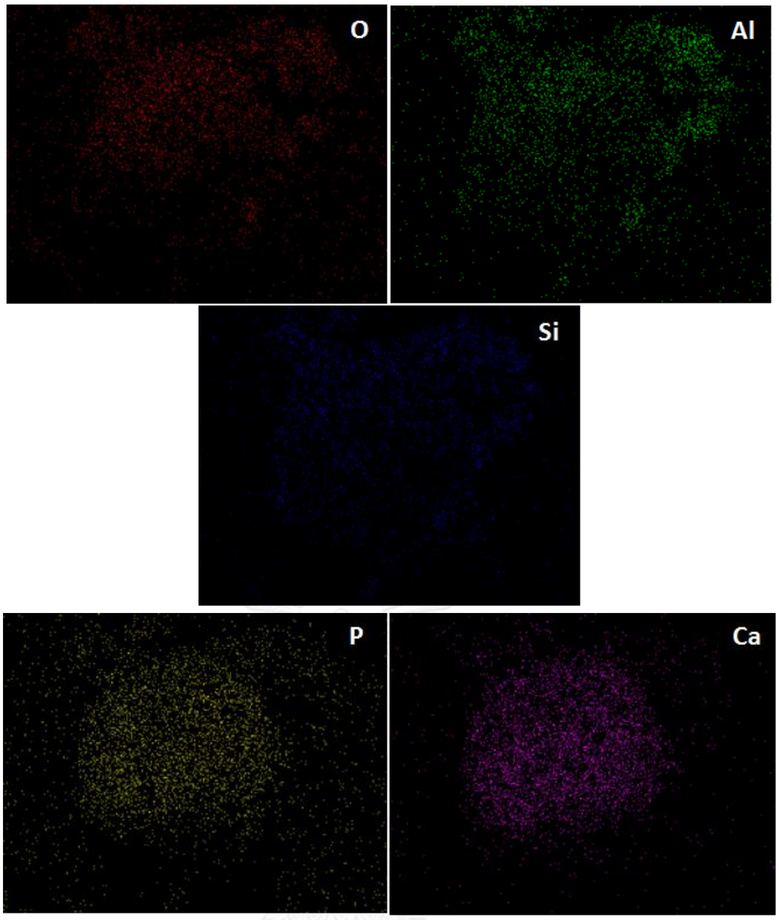

Figure 5. 16 The typical EDX mapping of 40H60AS-CS catalyst.

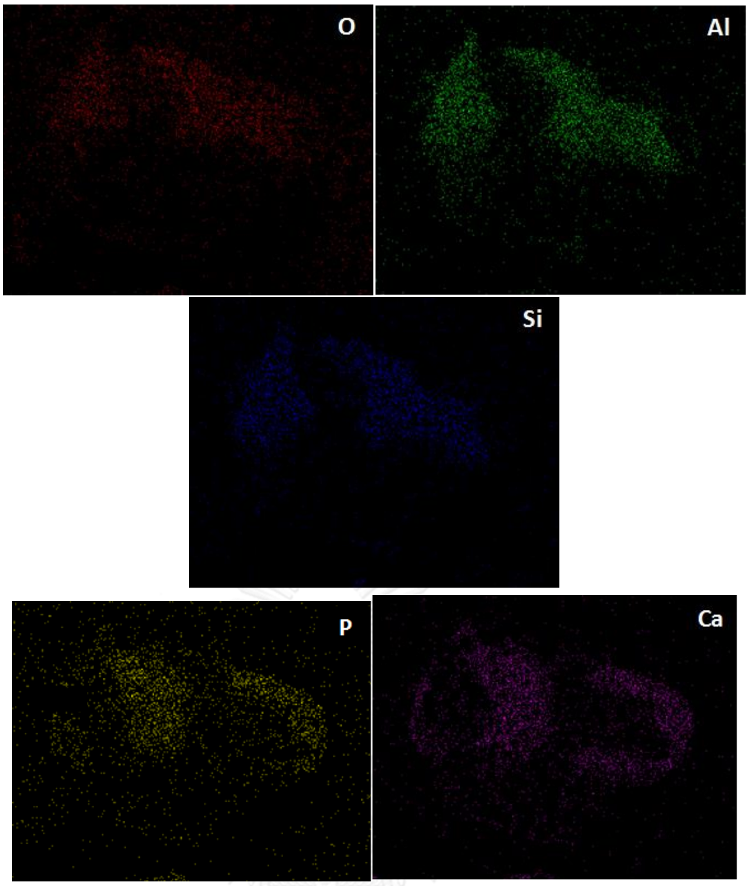

Figure 5. 17 The typical EDX mapping of 40H60AS-CP catalyst.

Figure 5.16 & 5.17 show dispersive the X-ray spectroscopy (EDX) analysis. All elements in 40H60AS-CS and 40H60AS-CP catalysts exhibit as dots spreading near surface of catalysts. Both of catalysts consists of Al, Si, O, Ca and P. All elements present well-distribution of elements on surface of catalysts.

The amount of each element on surface of both catalysts determining by EDX method is summarized in Table 5.6. The quantity of HAP on surface of 40H60AS-CS and 40H60AS-CP catalysts were 39% and 31%, respectively. The amount of HAP was approximate the number of its loading in catalyst preparation part.

Table 5. 6 The amount of each element on the surface of all catalysts from EDX.

Catalysts	**Amount of element on surface (wt%)**				
	Ca	P	Al	Si	O
40H60AS-CS	20.6	18.3	9.1	7.7	44.3
40H60AS-CP	17.8	13.2	14.6	8.2	46.2

5.2.1.4 Temperature programmed desorption (NH_3-TPD)

The acid property was measured by temperature-programmed desorption (NH_3-TPD). The surface acidity of 40H60AS-CS and 40H60AS-CP catalysts is aggregated in Table 5.7. The 40H60AS-CS and 40H60AS-CP catalysts present total acid site of 1,072.4 and 1,266.4 μ mol/g.cat, respectively. The amount of total acid of 40H60AS-CP catalyst is larger than 40H60AS-CS catalyst. Thus, 40H60AS-CP catalyst is possibly able to exhibit higher catalytic activity of ethanol dehydration reaction than 40H60AS-CS catalyst, due to the acid property is extremely important and has strong effect on dehydration reaction of ethanol. Moreover, 40H60AS-CP catalyst presents weak-modurate acid sites larger than 40H60AS-CS catalyst that is essential qualification of catalytic activity to produce DEE. Accordingly, 40H60AS-CP catalyst can produce DEE higher than 40H60AS-CS catalyst. Furthermore, both 40H60AS-CS and 40H60AS-CP catalysts prepared by chemical method exhibit the surface acidity larger than the 40H60AS-P catalyst prepared by physical method. Thereby, chemical method is a major way to prepare a suitable catalyst.

Table 5. 7 The surface acidity of all catalysts from NH_3-TPD.

Catalysts	**Number of acid sites (μ mol/g.cat)**			
	Weak acid sites	**Moderate acid sites**	**Strong acid sites**	**Total acid site**
40H60AS-CS	646.5	158.9	267.0	1,072.4
40H60AS-CP	558.9	350.2	357.3	1,266.4

The TPD profile of 40H60AS-CS and 40H60AS-CP catalysts is shown in Figure 5.18. Both catalysts present one desorption peak below 250°C that is assigned to weak acid site property. The quantity of weak acid-modurate site is related to results shown in Table 5.8 according to the area below curve. Modurate and strong acid sites occur at 250-400 and over 400°C, respectively. The amount of acid site rapidly decreased as seen in the Table. The amount of weak-modurate acid site is higher than strong acid site that is excellent characteristic to produce DEE.

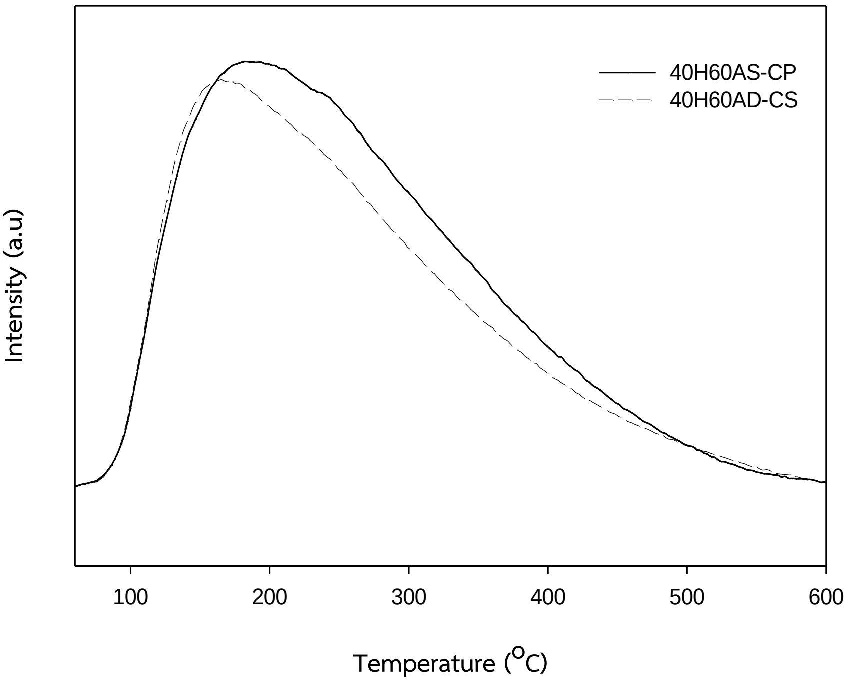

Figure 5. 18 NH_3-TPD profiles of all catalysts

5.2.1.5 X-Ray Fluorescence (XRF)

The quantitative results of 40H60AS-CS and 40H60AS-CP including Al-SSP and 40H60AS-P catalysts were measured by XRF. Chemical composition can be observed in Table 5.8. The major element of HAP were P and Ca and the main composition of Al-SSP were Al and Si including O. Al-SSP presented the composition of Al-SI weight ratio about 1. 40H60AS-P, 40H60AS-CS and 40H60AS-CP catalysts display weight ratio of HAP to Al-SSP around 0.4-0.8.

Table 5. 8 The composition in geological of all catalysts from XRF.

Catalysts	**Compound (wt%)**					
	Al_2O_3	**SiO_2**	**P_2O_5**	**CaO**	**Al/Si**	**[HAP/(Al/Si)]**
Al-SSP	51.0	49.0	-	-	1	-
40H60AS-P	36.4	31.1	12.1	20.4	1.2	0.5
40H60AS-CS	42.0	28.0	11.3	18.7	1.5	0.4
40H60AS-CP	32.8	19.6	18.8	28.8	1.6	0.8

5.2.1.6 Fourier Transform Infrared Spectroscopy (FTIR) Analysis

According to Figure 5.19 & 5.20 FTIR spectra of 40H60AS-CS and 40H60AS-CP catalysts were similar. Considering Figure 5.21, mostly characteristics of chemical groups in HAP are PO_4^{3-}, OH-, and CO_3^{2-}. The CO_3^{2-} group occurs at 2359, 1650 and 1459 cm^{-1}. A tiny sharp peak present at 600 wavenumber (cm^{-1}) represents a chemical group of PO_4^{3-}. The broad bands located at 3192, 3415 and 1649 cm^{-1} could be attributed to the O–H stretching vibration of hydroxyl group of HAP and/or hydrogen bonded-OH group as water molecule. For functional groups of alumina-silica, the Si-O-Si vibration was detected appearing the shoulder at 1026 cm^{-1}. The presence of Si-O-Al bonds around 1600-1700 cm^{-1}. A shoulder peak appears at 3629 cm^{-1} indicating the presence of Si-O. A band between Al=O of alumina-base occurs a sharp peak located at 1456 cm^{-1}.

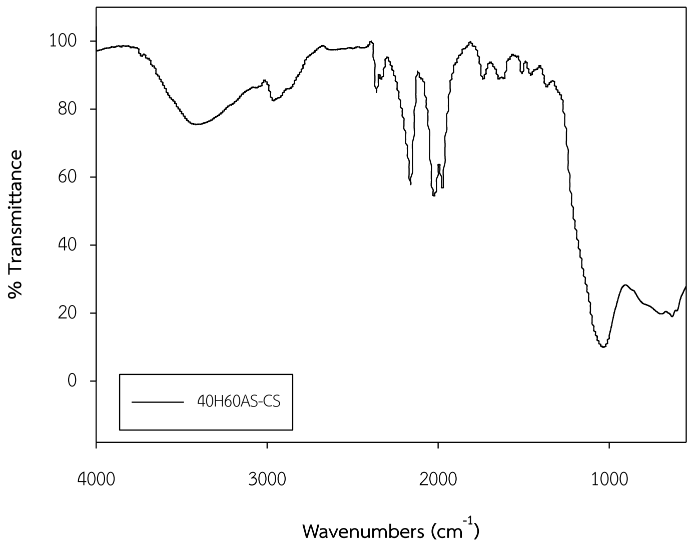

Figure 5. 19 FTIR spectra of 40H60AS-CS catalyst.

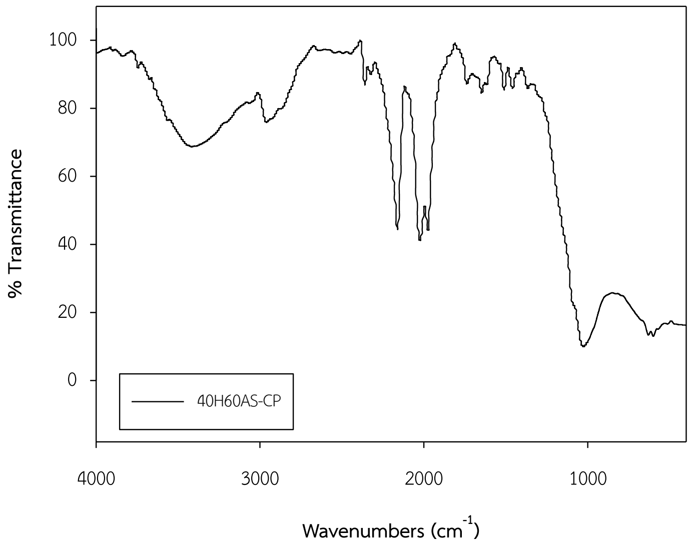

Figure 5. 20 FTIR spectra of 40H60AS-CP catalyst.

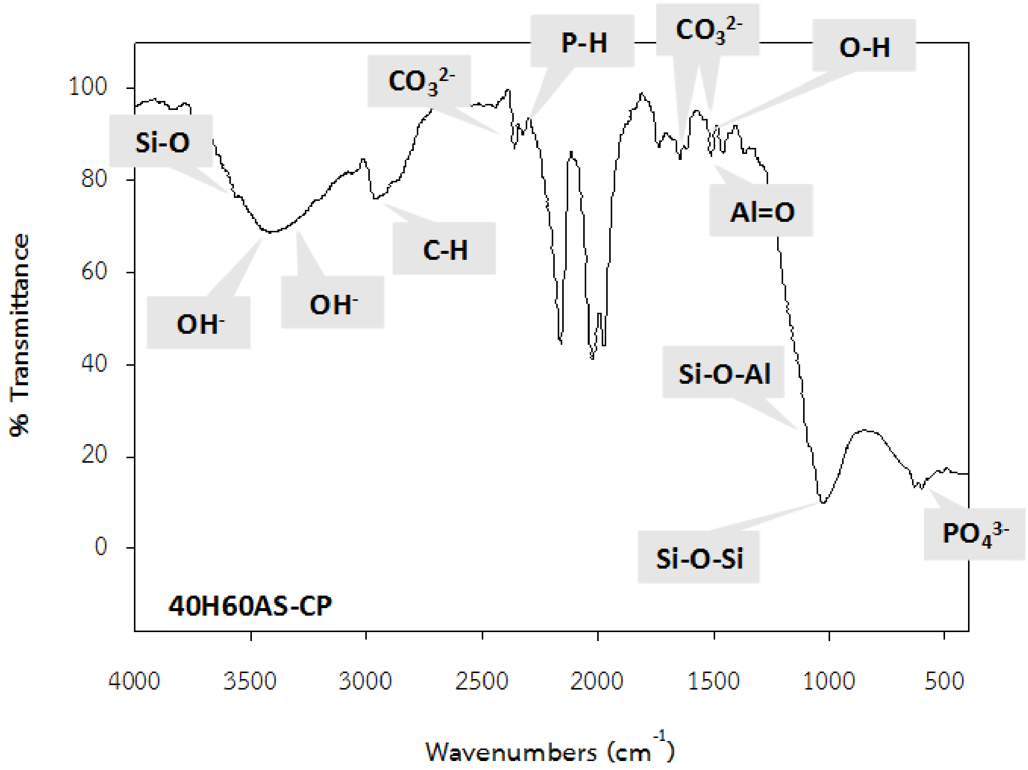

Figure 5. 21 FTIR spectra of 40H60AS-CP catalyst (display chemical groups).

Table 5. 9 The position of chemical groups of catalysts from FT-IR.

Chemical groups	absorption band (cm^{-1})	Description
PO_4^{3-}	500-600	v_4, bending mode
	1020-1120	v3, bending mode
P-H	957	low intensity broad peak
OH^-	3192	broad band stretching vibration & physically adsorbed water
	3450	-
CO_3^{2-}	1459	v_3
	1650	B-type
	2359	-
P-H	2457-2240	-
OH	1649,3300	vibration
Si-O-Si	1026	-
Si-O-Al	1069	lower side
H-O-H	1638	absorbed water molecules
Si–O	3629	-
Al=O	1456	-
C-H	2960	stretching (silica)

References: [30], [31], [32], [33], [34].

5.2.1.7 Raman spectroscopy

FT-Raman spectroscopy patterns of 40H60AS-CS and 40H60AS-CP catalysts are shown in Figure 5.22 & 5.23. The 40H60AS-CS and 40H60AS-CP catalysts exhibited quite similar pattern. Raman spectra of 40H60AS-CS catalyst is shown in Figure 5.22. A functional of PO_4^{3-} of HAP was observed at 463, 596 and 959 cm^{-1}. The sharp peak at 208 cm^{-1} was attributed to a band of calcium and phosphate. For alumina-silica, it shows only a band of silica and oxygen located at 587 cm^{-1}. Furthermore, the Raman spectra of 40H60AS-CP catalyst are shown in Figure 5.23. The specific characteristics of HAP showed a chemical groups of PO_4^{3-}, CO_3^{2-} and Ca-P. The observed bands at 606 and 1047 cm^{-1} were assigned to a functional group of PO_4^{3-} and CO_3^{2-} , respectively. A well-sharp peak at 959 displayed a band of phosphorus and oxygen including 1044 cm^{-1}. The weak band at 208 cm^{-1} was assigned to Ca-PO_4.

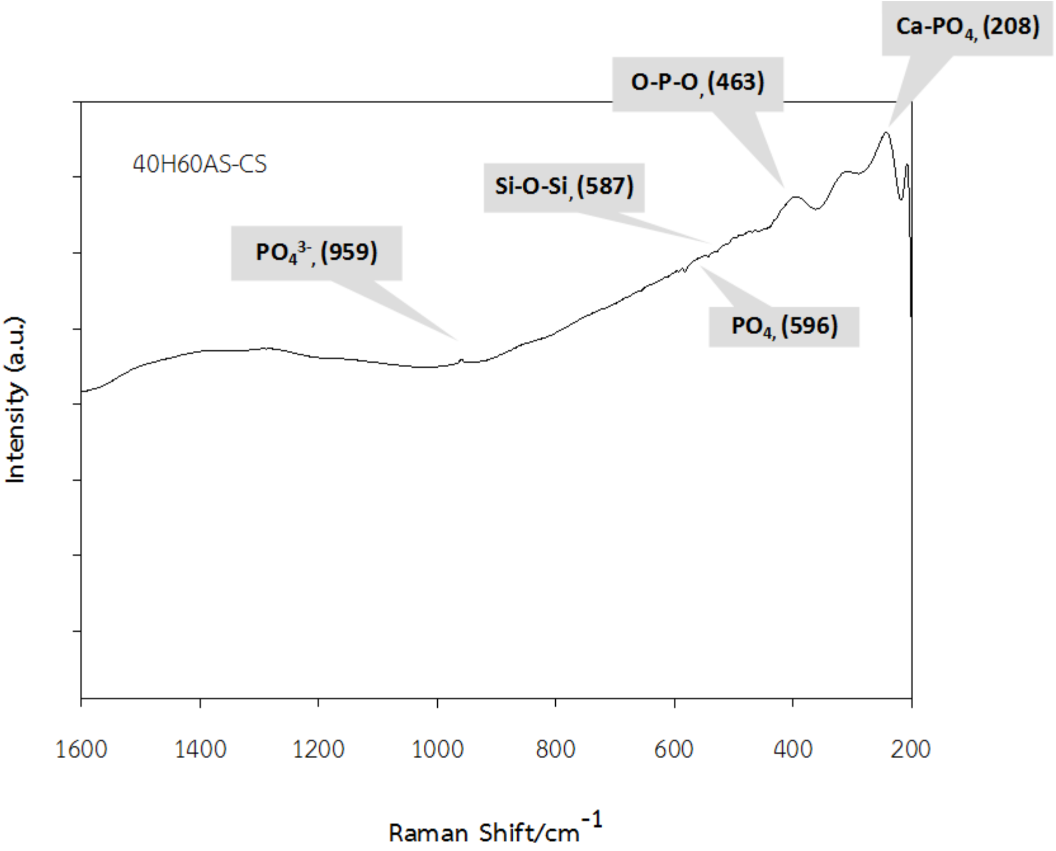

Figure 5. 22 FT-Raman spectra of 40H60AS-CS catalyst.

Table 5. 10 Raman band position of 40H60AS-CS catalyst.

Chemical groups	absorption band (cm^{-1})	Description
O-P-O	463	-
PO_4	587, 596	v_4
PO_4^{3-}	959	-
Ca-PO_4	208	weak band
Si-O-Si	587	-

References: [35], [36], [37], [38].

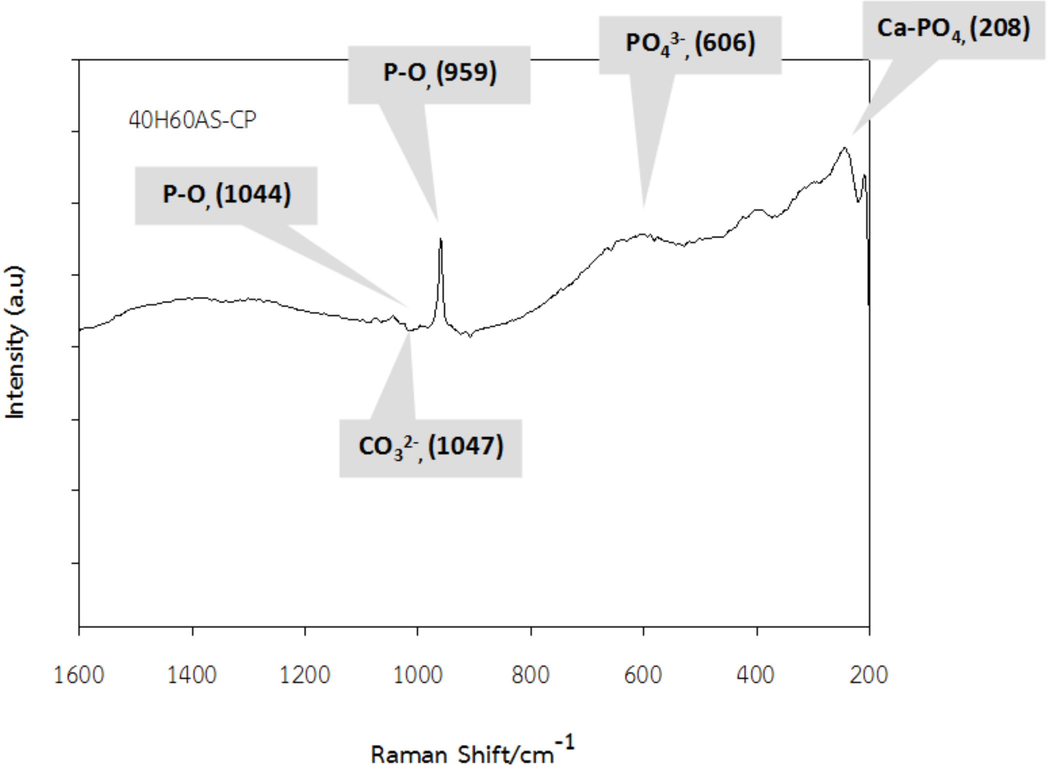

Figure 5. 23 FT-Raman spectra of 40H60AS-CP catalyst.

Table 5. 11 Raman band position of 40H60AS-CP catalyst.

Chemical groups	absorption band (cm^{-1})	Description
PO_4^{3-}	959	v_1, tetrahedral
P-O	1044	v_3
P-O	1074	v3, stretching
CO_3^{2-}	1074	-
Ca-PO_4	208	weak band
PO_4^{3-}	606	V_4

References: [35], [36], [37], [38].

5.2.2 Catalytic activity test

Both catalysts were tested for the catalytic activity in dehydration reaction of ethanol. 0.05 g of catalyst was added into continuous flow micro-reactor. First, the catalysts was treated by 60 ml/min of argon for one hour. Then, measuring in ethanol dehydration reaction in gas phase at atmospheric pressure between 200 to 400°C. All gas products were collected and determined by gas chromatograph with FID.

From experiment, the 40H60AS-CS catalyst conducted increased ethanol conversion with increasing reaction temperature. There was no significant ethanol conversion at temperature below 350°C for this catalyst. The ethanol conversion of 40H60AS-CP catalyst started at 300°C and continued increasing with enhancing the operating temperature. Owing to the quantification of 40H60AS-CP that exhibited larger BET surface area and surface acidity than those of 40H60AS-CS. Therefore, 40H60AS-CP catalyst can present catalytic activity of ethanol dehydration reaction at temperature lower than 40H60AS-CS catalyst. Both catalysts show the highest ethanol conversion at temperature of 400°C having ethanol conversion of 46% and 51%, respectively.

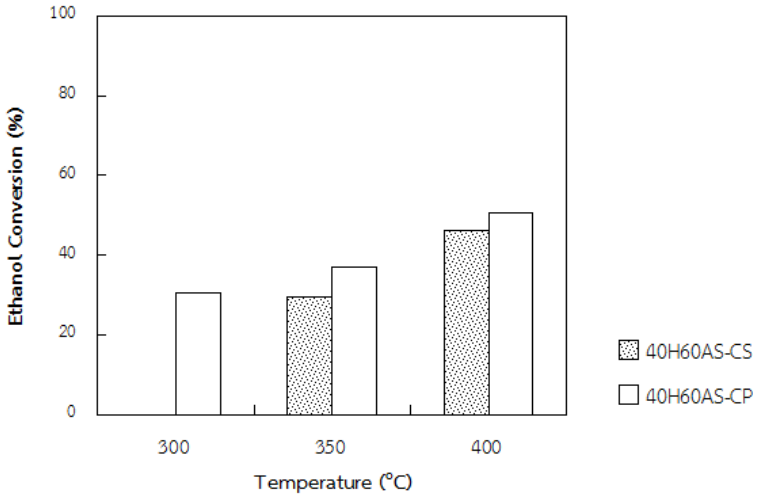

Figure 5. 24 Ethanol conversion of all catalysts at different temperatures.

The highest DEE selectivity is obtained at 300°C by 40H60AS-CP catalyst and decreased while reaction temperature was increased. 40H60AS-CP catalyst exhibited the highest DEE selectivity of 79% at 300°C, due to the amount of weak-moderate acid sites of 40H60AS-CP catalyst that affected on DEE selectivity on during ethanol dehydration reaction. The DEE selectivity of 40H60AS-CS occurred at temperature of 350°C and depreciated with higher operating temperature. Comparison both catalysts, at lower temperature (300°C) only 40H60AS-CP catalyst can give DEE selectivity, while 40h60AS-CS catalyst cannot. This is because of its acid property that significant and militarily important in order to produce DEE.

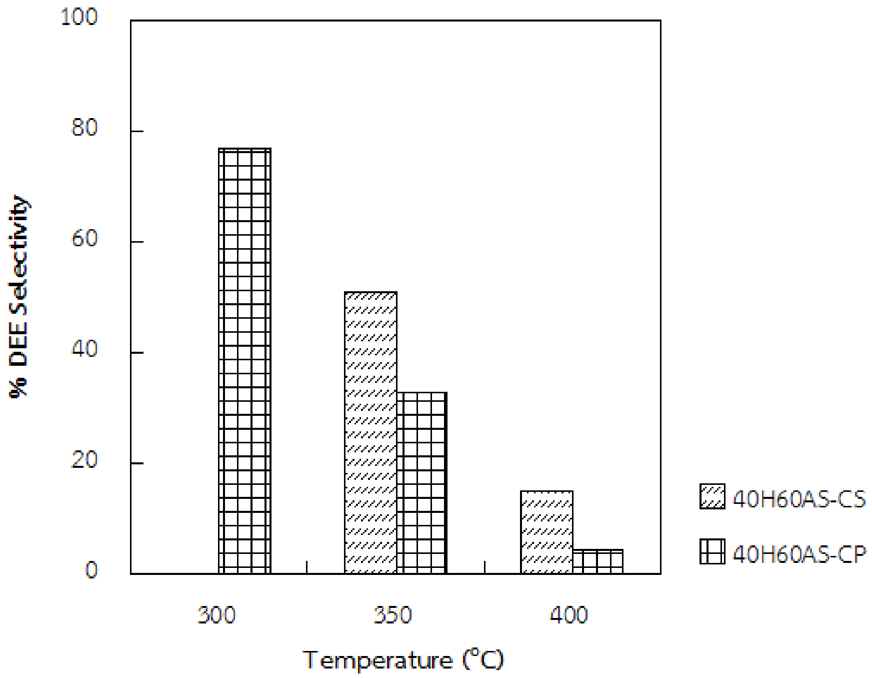

Figure 5. 25 DEE selectivity of all catalysts at different temperatures.

The DEE production of 40H60AS-CS and 40H60AS-CP catalysts are concluded in Table 5.12. The 40H60AS-CS catalyst exhibited the highest DEE yield as 15% at 350°C. At 300°C, 40H60AS-CP catalyst exhibited the highest DEE yield as 24%. Thus, the 40H60AS-CP catalyst has catalytic activity higher than 40H60AS-CS catalyst that related to their characteristics for both BET surface area and acid quantification. Considering catalysts prepared by chemical and physical methods, although DEE yield obtained from the 40H60AS-CP catalyst is lower that of 40H60AS-P catalyst, it can be operated at lower temperature. This is the result of their properties. The 40H60AS-CP catalyst has larger BET surface area and total surface acidity than 40H60AS-P catalyst 1.9 and 1.7 times, respectively.

Table 5. 12 Product yield of all catalysts obtained from ethanol dehydration.

Catalysts	**% Yield (300°C)**		**% Yield (350°C)**		**% Yield (400°C)**	
	DEE	**Ethylene**	**DEE**	**Ethylene**	**DEE**	**Ethylene**
40H60AS-CS	0	0	15.1	14.5	6.9	39.3
40H60AS-CP	23.5	7.1	12.1	24.8	2.2	48.4

5.3 Investigation of catalytic activity of HAP/Al-SSP catalysts for time-on-stream (TOS) during 10 hours.

In order to produce DEE, suitable condition must be focused, DEE production is required low temperature following thermodynamic properties. From previous experiment, the highest DEE yield was obtained by suitable condition. The 40H60AS-CS and 40H60AS-P catalysts exhibited the highest DEE yield at 350°C. The 40H60AS-CP catalyst presented the highest DEE yield at 300°C. This was the suitable temperature for ethanol dehydration to produce high yield of DEE. The catalytic activity of all catalysts was determined under time on stream for ten hours at each suitable temperature. According to Figure 5.26, the highest ethanol conversion during time on stream for ten hours was obtained from 40H60AS-P catalyst, while 40H60AS-CP catalyst was lower and 40H60AS-CS was the lowest. Although 40H60AS-P catalyst presented ethanol conversion larger than 40H60AS-CP catalyst, the 40H60AS-CP catalyst was operated at lower temperature. All catalysts can maintain ethanol conversion during ten hours on dehydration reaction of ethanol.

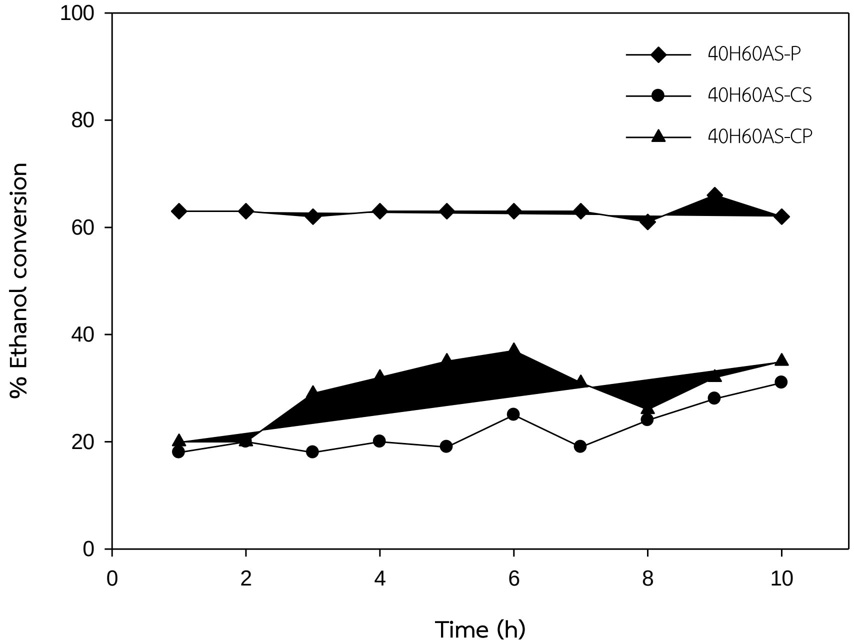

Figure 5. 26 Ethanol conversion of all catalysts for time on stream 10 h.

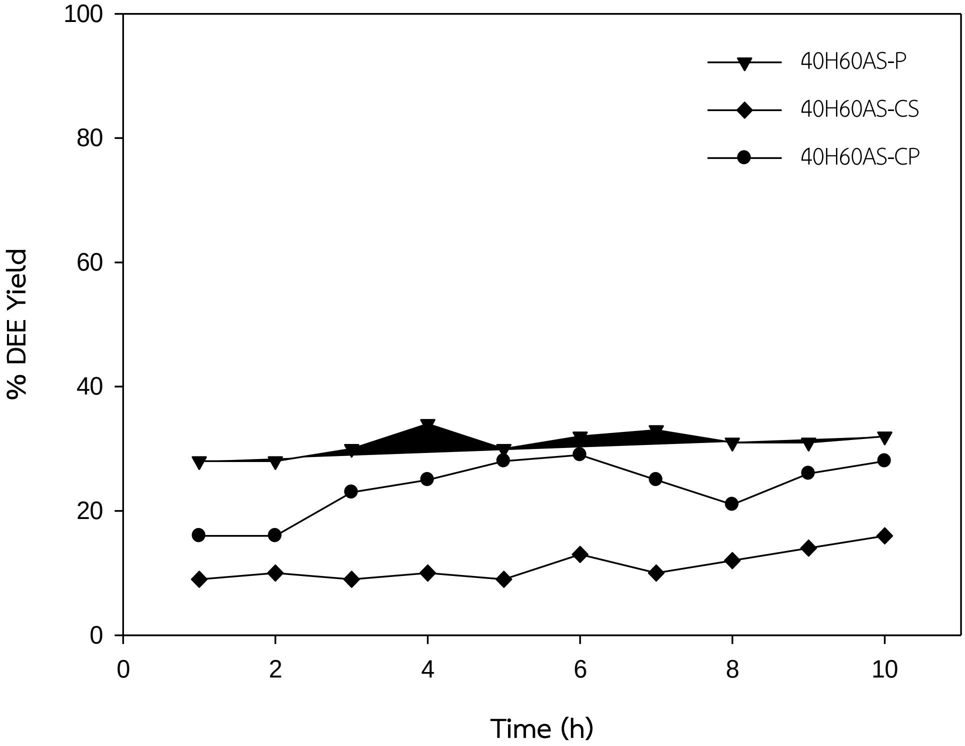

Figure 5. 27 DEE yield of all catalysts for time on stream 10 h.

Considering DEE yield, the results are shown in Figure 5.27. DEE yield stably obtained during ten hours from all catalysts. The highest DEE yield incurred by 40H60AS-P catalyst as 30%. Even if the 40H60AS-P catalyst gives the highest DEE yield, it is too low value when compared with the ethanol conversion. This is because of its low DEE selectivity. Moreover, average DEE yield obtained by 40H60AS-CP catalyst was similar to 40H60AS-P catalyst due to all catalysts were operated at low temperature and DEE yields were also low.

In order to determine the amount of coke content in catalysts. TGA technique was performed. All catalysts exhibited similar behavior after using in ethanol dehydration reaction. According to Figure 5.28 and 5.29, all catalysts show rapid weight loss at temperature below 100°C. This results from deposition of water on surface of catalysts. At high temperature (200-800°C), the weight loss was the burning of coke implanted on surface of catalyst after running in ethanol dehydration. Considering the highest weight loss of 40H60AS-CP. It is due to this catalyst has the highest total acid sites among other catalysts. It demonstrated the distinctness of surface acidity quantity of catalysts. Based on the study, 40H60AS-CP catalyst is perhaps a good choice for DEE production, even though DEE yield was less than that of 40H60AS-P catalyst. However, it can be operated at lower reaction temperature that requires lower energy of production process.

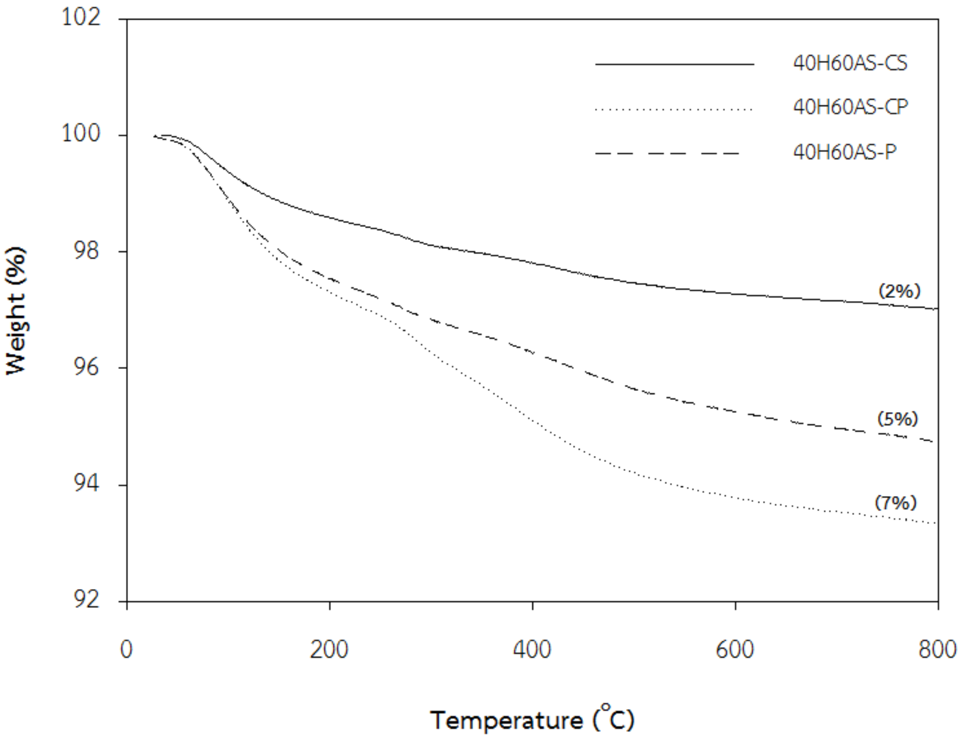

Figure 5. 28 Thermal gravimetric analysis (TGA) of spent catalysts for time on stream during 10 hours.

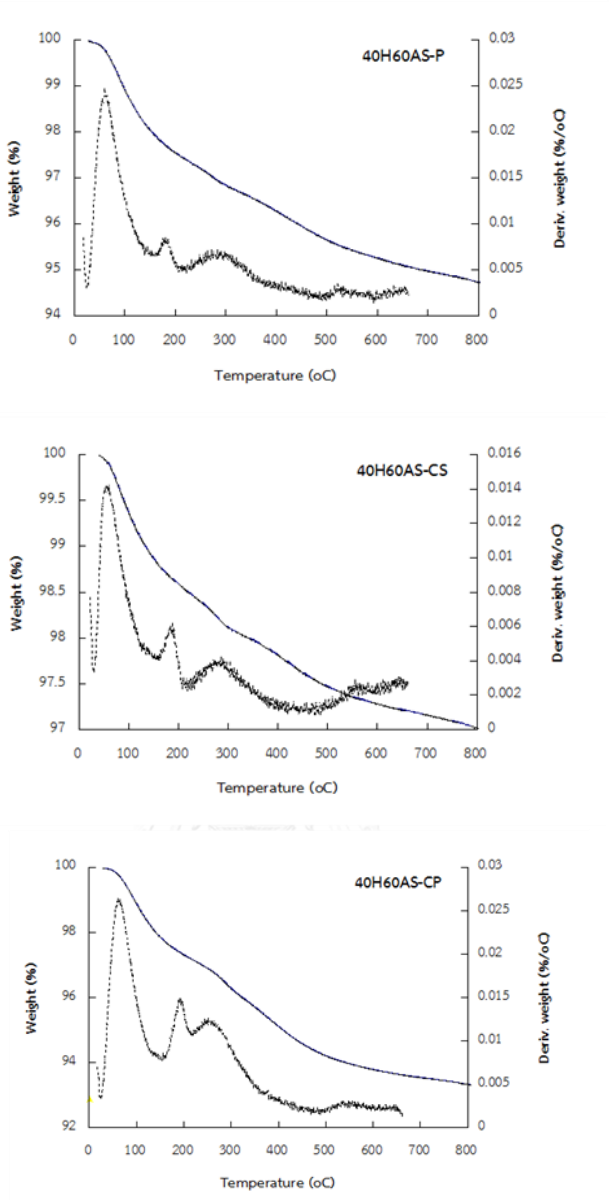

Figure 5. 29 Thermogravimetric and differential thermal analysis of spent catalysts for time on stream during 10 hours.

From previous research, DEE product does not obtain from any catalysts at temperature of 350°C. According to Chatchawanrat S. (2013) [39], activated carbon catalyst exhibited only acetaldehyde and ethylene production at temperature range from 200 to 400°C. The DEE selectivity can immediately decrease at temperature 200 to 250°C from pure alumina-silica catalyst. Although, there are a higher total acid site more than HAP/Al-SSP catalysts [40]. It is shown that HAP catalyst can inhibit ethylene production at high temperature (350°C) and DEE can be obtained from HAP/Al-SSP catalyst. H-beta zeolite and HAP/Al-SSP (40H60AS-CP) catalyst presented similar DEE production, although H-beta zeolite catalyst displayed a higher weak and total acid sites. At temperature of 350°C, H-beta zeolite and alumina-base catalysts rarely exhibited DEE yield [41]. This confirms that HAP catalyst gives a good catalytic activity for ethanol dehydration in order to produce DEE at high temperature (350°C).

CHAPTER 6

CONCLUSIONS AND RECOMMENDATIONS

In this study, catalysts were divided into two preparation parts; physical and chemical mixing method. We study all catalysts including characteristics and catalytic activity via ethanol dehydration reaction. Considering effect of amount of hydroxyapatite (HAP) and alumina-silica on the catalytic activity including various preparation methods for catalysts (sol-gel and co-precipitation methods). The summary of overall study is shown in this chapter.

6.1 Conclusions

1. Considering effect of amount of hydroxyapatite and alumina-silica catalyst on the catalytic activity of ethanol dehydration reaction. The 40H60AS-P catalyst gives the highest DEE yield at low temperature (350°C) because it has the largest amount of surface acidity of weak-moderate acid sites.

2. For comparison the catalytic activity of catalysts prepared by sol-gel and co-precipitation mixing method, it was found that the co-precipitation method gives better catalytic activity. The DEE yield was obtained at 300°C for 24% from 40H60AS-CP catalyst. This is probably due to its larger BET surface area and total amount of acid sites.

3. The catalytic performance was investigated in time-on-stream for ten hours. Three catalysts (40H60AS-P, 40H60AS-CS and 40H60AS-CP) can maintain their ethanol conversion and catalytic activity of each optimal temperature.

4. Comparison the catalytic activity for DEE production of three catalysts (40H60AS-P, 40H60AS-CS and 40H60AS-CP) is as shown in Table 6.

Table 6. 1 Product yield of all catalysts obtained from ethanol dehydration.

Catalysts	**% Yield (300°C)**		**% Yield (350°C)**		**% Yield (400°C)**	
	DEE	**Ethylene**	**DEE**	**Ethylene**	**DEE**	**Ethylene**
40H60AS-P	0	0	32.1	23.0	27.6	55.9
40H60AS-CS	0	0	15.1	14.5	6.9	39.3
40H60AS-CP	23.5	7.1	12.1	24.8	2.2	48.4

According to Table 6, the 40H60AS-CP catalyst is the best catalyst for DEE production. It gives the highest DEE yield at lower temperature (300°C) due to it has the highest BET surface area and total surface acidity.

6.2 Recommendations

Following by literature review, the acid property is strongly important for ethanol dehydration reaction. In order to improve the catalytic activity and DEE production, catalysts must have a large BET surface area and surface acidity for higher catalytic activity at low temperature. We propose recommendation as follows:

- To improve DEE production and catalytic activity at low temperature by various impregnation of metals, such as ruthenium and zinc-oxide that can improve strong acid site.
- In order to improve basic site of catalyst for acetaldehyde production, palladium, platinum or strontium should be further investigated.

REFERENCES

[1] Bailey, B. Diethyl Ether (DEE) as a Renewable Diesel Fuel. National Renewable Energy Laboratory.

[2] Górski, K. and Przedlacki, M. Evaluation of the Influence of Diethyl Ether (DEE) Addition on Selected Physicochemical Properties of Diesel Oil and Ignition Delay Period. Energy & Fuels 28(4) (2014): 2608-2616.

[3] Goutham Solasa, N.S.S., T.Raghu Krishna Prasad, G.Suresh Babu. Diesel Engine Perormance Improvement by Using Cetane Improver International Journal of Engineering and Advanced Technology (IJEAT) 2(4).

[4] Alharbi, W., Brown, E., Kozhevnikova, E.F., and Kozhevnikov, I.V. Dehydration of ethanol over heteropoly acid catalysts in the gas phase. Journal of Catalysis 319 (2014): 174-181.

[5] Rahmanian, A. and Ghaziaskar, H.S. Continuous dehydration of ethanol to diethyl ether over aluminum phosphate–hydroxyapatite catalyst under sub and supercritical condition. The Journal of Supercritical Fluids 78 (2013): 34-41.

[6] Ghantani, V.C., Lomate, S.T., Dongare, M.K., and Umbarkar, S.B. Catalytic dehydration of lactic acid to acrylic acid using calcium hydroxyapatite catalysts. Green Chemistry 15(5) (2013): 1211.

[7] Yan, B., Tao, L.-Z., Liang, Y., and Xu, B.-Q. Sustainable Production of Acrylic Acid: Catalytic Performance of Hydroxyapatites for Gas-Phase Dehydration of Lactic Acid. ACS Catalysis 4(6) (2014): 1931-1943.

[8] Tsuchida, T., Sakuma, S., Takeguchi, T., and Ueda, W. Direct Synthesis ofn-Butanol from Ethanol over Nonstoichiometric Hydroxyapatite. Industrial & Engineering Chemistry Research 45(25) (2006): 8634-8642.

[9] Tsuchida, T., Yoshioka, T., Sakuma, S., Takeguchi, T., and Ueda, W. Synthesis of Biogasoline from Ethanol over Hydroxyapatite Catalyst. Industrial & Engineering Chemistry Research 47(5) (2008): 1443-1452.

[10] Doheim, M.M., Hanafy, S.A., and El-Shobaky, G.A. Catalytic conversion of ethanol and isopropanol over the Mn2O3/Al2O3 system doped with Na2O. Materials Letters 55(5) (2002): 304-311.

[11] Luts, T. and Katz, A. Chemisorption and Dehydration of Ethanol on Silica: Effect of Temperature on Selectivity. Topics in Catalysis 55(1-2) (2012): 84-92.

[12] Pérez, L.L., Zarubina, V., Mayoral, A., and Melián-Cabrera, I. Silica promoted self-assembled mesoporous aluminas. Impact of the silica precursor on the structural, textural and acidic properties. Catalysis Today 250 (2015): 115-122.

[13] Phung, T.K. and Busca, G. Ethanol dehydration on silica-aluminas: Active sites and ethylene/diethyl ether selectivities. Catalysis Communications 68 (2015): 110-115.

[14] Chanchuey, T., Autthanit, C., and Jongsomjit, B. Effect of Mo-Doped Mesoporous Al-SSP Catalysts for the Catalytic Dehydration of Ethanol to Ethylene. Journal of Chemistry 2016 (2016): 1-8.

[15] Fan, D., Dai, D.-J., and Wu, H.-S. Ethylene Formation by Catalytic Dehydration of Ethanol with Industrial Considerations. Materials 6(1) (2012): 101-115.

[16] Yasushi Suetsugu, T.T. Implants and biomaterials (hydroxyapatite) Chief Researcher of Biomaterials Center, National Institute for Materials Science.

[17] Nidhi Kantharia, S.N., Sanjay Apte, Mohit Kheur, Supriya Kheur, Bharat Kale. Nano-hydroxyapatite and its contemporary applications. Journal of Dental Research and Scientific Development 1(1) (2014): 15-19.

[18] KOLTHOFF, I.M. “THEORY OF COPRECIPITATION.” THE FORMATION AND PROPERTIES OF CRYSTALLINE PRECIPITATES. 862-881.

[19] Kim, Y.T., Jung, K.-D., and Park, E.D. Gas-phase dehydration of glycerol over silica–alumina catalysts. Applied Catalysis B: Environmental 107(1-2) (2011): 177-187.

[20] Phung, T.K., Lagazzo, A., Rivero Crespo, M.Á., Sánchez Escribano, V., and Busca, G. A study of commercial transition aluminas and of their catalytic activity in the dehydration of ethanol. Journal of Catalysis 311 (2014): 102-113.

[21] Ogo, S., Onda, A., Iwasa, Y., Hara, K., Fukuoka, A., and Yanagisawa, K. 1-Butanol synthesis from ethanol over strontium phosphate hydroxyapatite catalysts with various Sr/P ratios. Journal of Catalysis 296 (2012): 24-30.

[22] Matsuura, Y., Onda, A., Ogo, S., and Yanagisawa, K. Acrylic acid synthesis from lactic acid over hydroxyapatite catalysts with various cations and anions. Catalysis Today 226 (2014): 192-197.

[23] Sudhakar, M., Kumar, V.V., Naresh, G., Kantam, M.L., Bhargava, S.K., and Venugopal, A. Vapor phase hydrogenation of aqueous levulinic acid over hydroxyapatite supported metal (M=Pd, Pt, Ru, Cu, Ni) catalysts. Applied Catalysis B: Environmental 180 (2016): 113-120.

[24] Kiyoshi Okada, T.T., Yoshikazu Kameshima, Atsuo Yasumoria and Kenneth J. D. MacKenzie. Porous properties of coprecipitated Al2O3–SiO2 xerogels prepared from aluminium nitrate nonahydrate and tetraethylorthosilicate. J. Mater. Chem., 9 (1999): 1307–1312.

[25] Granados-Correa, F., Vilchis-Granados, J., Jiménez-Reyes, M., and Quiroz-Granados, L.A. Adsorption Behaviour of La(III) and Eu(III) Ions from Aqueous Solutions by Hydroxyapatite: Kinetic, Isotherm, and Thermodynamic Studies. Journal of Chemistry 2013 (2013): 1-9.

[26] <49_2_Philadelphia_10-04_1181.pdf>.

[27] Krutpijit, C. and Jongsomjit, B. Catalytic Ethanol Dehydration over Different Acid-activated Montmorillonite Clays. J Oleo Sci 65(4) (2016): 347-55.

[28] Cecilia, J.A., García-Sancho, C., Mérida-Robles, J.M., Santamaría-González, J., Moreno-Tost, R., and Maireles-Torres, P. V and V–P containing Zr-SBA-15 catalysts for dehydration of glycerol to acrolein. Catalysis Today 254 (2015): 43-52.

[29] Lee, D.S.H., Pai, Y., and Chang, S. Effect of Thermal Treatment of the Hydroxyapatite Powders on the Micropore and Microstructure of Porous Biphasic Calcium Phosphate Composite Granules. Journal of Biomaterials and Nanobiotechnology 04(02) (2013): 114-118.

[30] Stark, e.a. FLAME SYNTHESIS OF METAL SALT NANOPARTICLES, IN PARTICULAR CALCIUM AND PHOSPHATE COMPRISING NANOPARTICLES. United States Patent US 7,879,303 B2 (2011).

[31] Gangwar, J., Gupta, B.K., Tripathi, S.K., and Srivastava, A.K. Phase dependent thermal and spectroscopic responses of Al2O3 nanostructures with different morphogenesis. Nanoscale 7(32) (2015): 13313-44.

[32] Ereiba, K.M.T., Mostafa, A.G., Gamal, G.A., and Said, A.H. In vitro study of iron doped hydroxyapatite. Journal of Biophysical Chemistry 04(04) (2013): 122-130.

[33] Kumar, R., Prakash, K.H., Cheang, P., Gower, L., and Khor, K.A. Chitosan-mediated crystallization and assembly of hydroxyapatite nanoparticles into hybrid nanostructured films. J R Soc Interface 5(21) (2008): 427-39.

[34] CHTAINI, M.A.E.M.a.A. Electrochemical Studies of Adsorption of Paraquat onto Ca10(PO4)6(OH)2 from Aqueous Solution. Leonardo Journal of Sciences (12) (2008): 25-34.

[35] Ciobanu, C.S., Iconaru, S.L., Le Coustumer, P., and Predoi, D. Vibrational Investigations of Silver-Doped Hydroxyapatite with Antibacterial Properties. Journal of Spectroscopy 2013 (2013): 1-5.

[36] Yilmaz, B. and Evis, Z. Raman Spectroscopy Investigation of Nano Hydroxyapatite Doped with Yttrium and Fluoride Ions. Spectroscopy Letters 47(1) (2013): 24-29.

[37] Wachs, M.A.V.a.I.E. In Situ Raman Spectroscopy of Alumina-Supported Metal Oxide Catalysts. Zettlemoyer Center for Surface Studies and Department of Chemical Engineering, Lehigh University 96 (1992): 5008-5016

[38] Magg, N. Vibrational spectra of alumina- and silica-supported vanadia revisited: An experimental and theoretical model catalyst study. Journal of Catalysis 226(1) (2004): 88-100.

[39] Naresh, G. DEHYDROGENATION OF ETHANOL TO ACETALDEHYDE OVER ACTIVATED CARBON CATALYSTS. Chulalongkorn University (2013).

[40] Chanchuey, T. THE ETHANOL DEHYDRATION OVER AL-SI COMPOSITE CATALYSTS Chulalongkorn University (2013).

[41] Kamsuwan, T. DEHYDRATION REACTION OF ETHANOL OVER BETA ZEOLITE CATALYST Chulalongkorn University (2015).

APPENDIX

APPANDIX A

CALCULATION FOR ACID SITES OF CATALYSTS

The acidity was measured by NH_3-TPD, it can be calculated from NH3-TPD profile as follows;

Acidity of catalysts = (mole of NH_3 desorption)/(amount of dry catalyst) -------- equation (B.1)

To Calculate mole of NH3 desorption from the calibration curve of NH3 as follow:

NH_3 desorption (mole) = 0.0003 x A

Where, A is area under peak of the NH_3-TPD profile.

And then, we denote amount of dry catalyst as B (g.). So the equation (B.1) can be take place as equation (B.2)

Acidity of catalysts = (0.003 × A)/B ----------------------- equation (B.2)

APPANDIX B
CALIBRATION CURVE

Calibration curves were used calculation mole of ethanol, ethylene, DEE and acetaldehyde as shown in Figure C.1-C.4. The concentration of these were analyzed by the gas chromatography Shimadzu model 14A, capillary column DB-5 of flame ionization detector (FID). The conditions uses in GC are presented in Table C.1

Table C. 1 Conditions use in GC-14A.

PARAMETERS	CONDITION
WIDTH	5
SLOPE	100
DRIFT	0
MIN.AREA	300
T.DBL	1000
STOP TIME	8 min
ATTEN	2
SPEED	3
METHOD	Normalization
SPL.WT	100
IS.WT	1

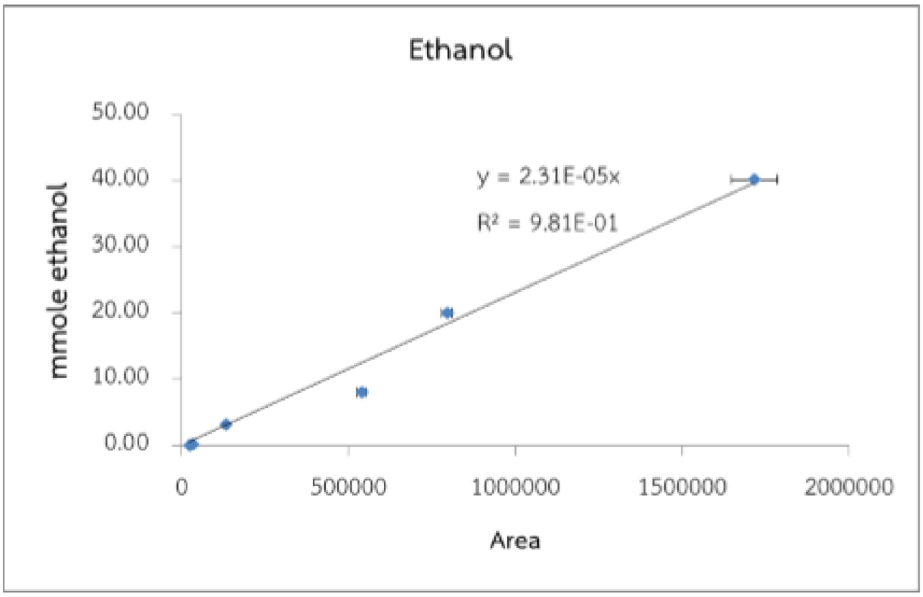

Figure C.1 The calibration curve of ethanol.

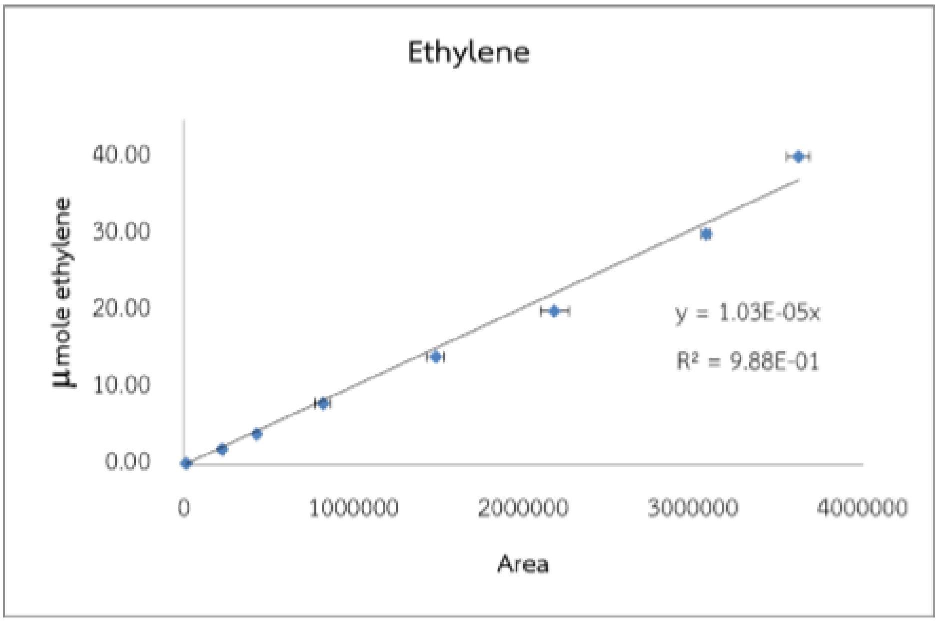

Figure C.2 The calibration curve of ethylene.

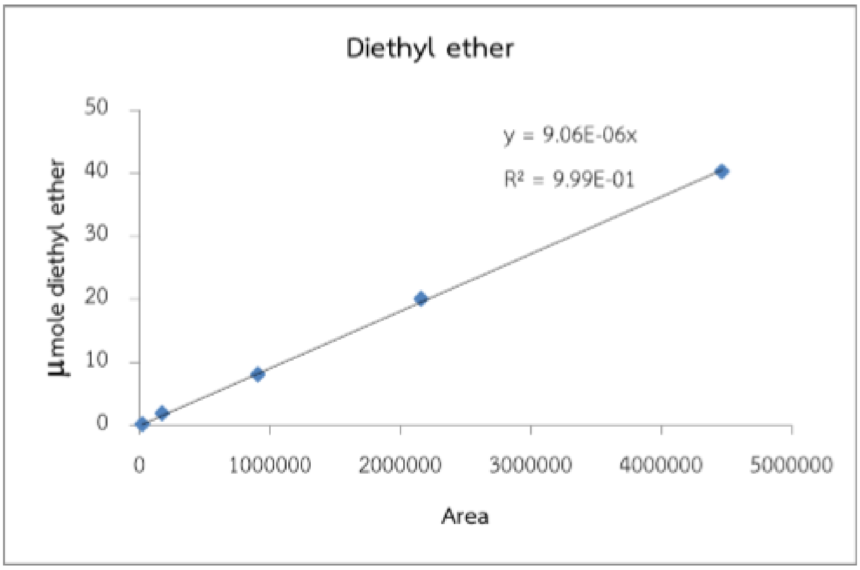

Figure C.3 The calibration curve of DEE.

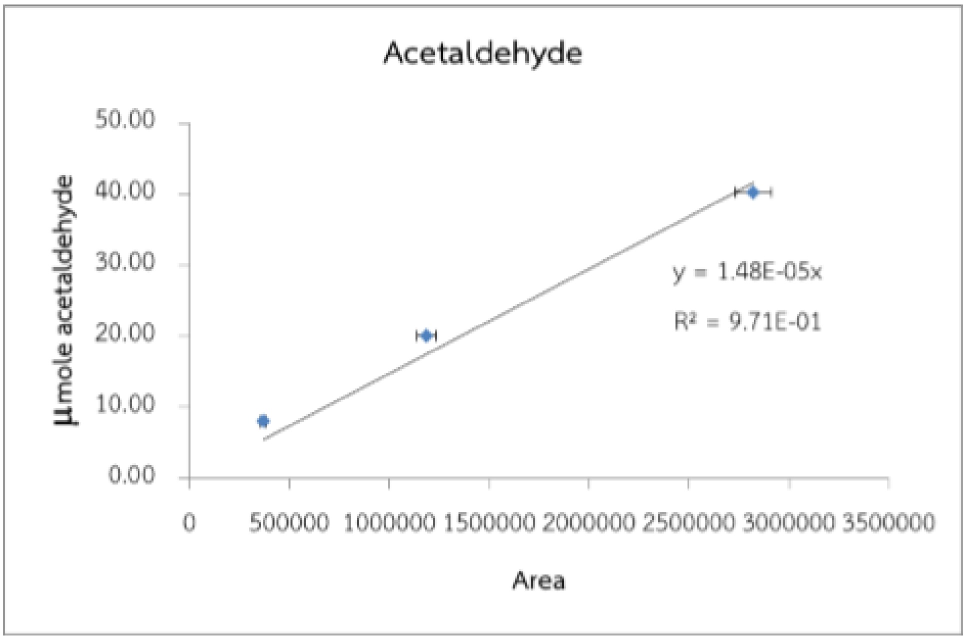

Figure C.4 The calibration curve of acetaldehyde.

APPANDIX C

CONVERSION, SELECTIVITY AND YIELD

The catalytic performance for the ethanol conversion was evaluated in term of activity for ethanol conversion.

$$\text{Ethanol conversion (\%)} = \frac{\text{(mole of ethanol in feed - mole of ethanol in product)} \times 100}{\text{mole of ethanol in feed}}$$

Products selectivity are defined as moles of products converted with respect to product in out of reaction as follows:

$$\text{Ethylene selectivity (\%)} = \frac{\text{mole of ethylene in product} \times 100}{\text{mole of total products}}$$

$$\text{Diethyl ether selectivity (\%)} = \frac{\text{mole of DEE in product} \times 100}{\text{mole of total products}}$$

$$\text{Acetaldehyde selectivity (\%)} = \frac{\text{mole of acetaldehyde in product} \times 100}{\text{mole of total products}}$$

Where: Total product is mole of (Ethylene + DEE + Acetaldehyde).

Products yield was evaluated in term of ethanol conversion and products selectivity

Ethylene yield (%) = (ethylene selectivity × ethanol conversion)/100

DEE yield (%) = (DEE selectivity × ethanol conversion)/100

Acetaldehyde yield (%) = (acetaldehyde selectivity × ethanol conversion)/100

From calibration curve;

Mole of ethanol = (2.31×10^{-5}) x area

Mole of ethylene = (1.03×10^{-5}) x area

Mole of diethylether = (9.06×10^{-6}) x area

Mole of acetaldehyde = (1.48×10^{-5}) x area

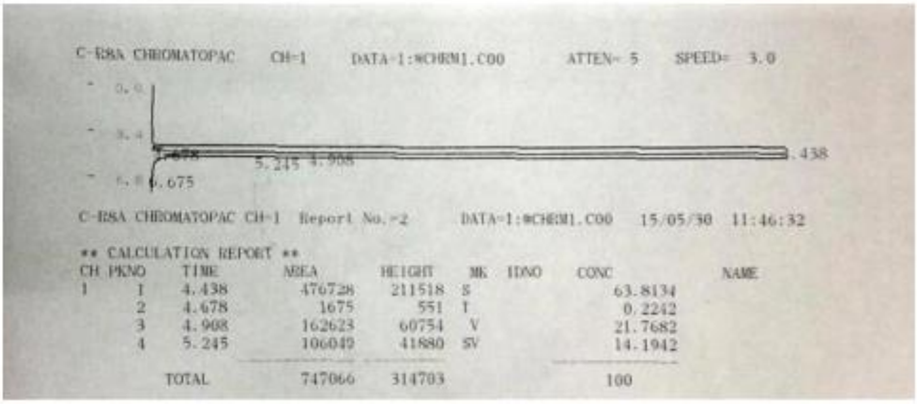

```
C-R8A CHROMATOPAC    CH=1    DATA-1:#CHRM1.C00      ATTEN= 5    SPEED= 3.0

C-R8A CHROMATOPAC CH=1  Report No.=2      DATA=1:#CHRM1.C00   15/05/30  11:46:32

** CALCULATION REPORT **
CH PKNO    TIME        AREA      HEIGHT   MK  IDNO    CONC             NAME
1     1    4.438     476728     211518   S               63.8134
      2    4.678       1675        551   T                0.2242
      3    4.908     162623      60754    V              21.7682
      4    5.245     106049      41880   SV              14.1942
                   ---------- ----------           ------------
         TOTAL       747066     314703                  100
```

Figure D.1 The GC result

Example;

From Figure D.1, the area of reactant and product can be detected by gas chromatography. The peak at 4.438 minute shown area of ethylene, while peak at 4.678, 4.908 and 5.245 minute represented area of acetaldehyde, ethanol and diethylether, respectively.

So, mole of ethanol = (2.31x10-5) x 162623

= 3.76 mole

APPANDIX D
LIST OF PUBLICATION

Proceeding

Auemporn Mongkolserm and Bunjerd jongsomjit, “Production of Diethylether by Catalytic Dehydration of Ethanol over the Hydroxyapatite (HAP) Solid Acid Catalyst” Proceeding of the PACCON 2016, BITEC Bangkok, Thailand, January 9-11, 2016.

VITA

Miss Auemporn Mongkolserm was born on October 17, 1991 in Chonburi, Thailand. She graduated high school from Rayongwittayakom school in 2009 and received the Bachelor’s Degree of Science from the Department of Chemical Technology, Faculty of Science, Chulalongkorn University (CU) in April 2014. She continued the Master of Engineering in Chemical Engineering, Chulalongkorn University (CU) in August 2014.